Environmental Research 214 (2022) 113731

Contents lists available at ScienceDirect

Environmental Research

journal homepage: www.elsevier.com/locate/envres

Transition metal oxides with perovskite and spinel structures for electrochemical energy production applications

J.X. Flores-Lasluisa [a], F. Huerta [b], D. Cazorla-Amorós [c], E. Morallón [a,*]

[a] Dept. Química Física e Instituto Universitario de Materiales, Universidad de Alicante, Ap. 99, E-03080, Alicante, Spain
[b] Dept. Ingenieria Textil y Papelera, Universitat Politecnica de Valencia, Plaza Ferrandiz y Carbonell, 1, E-03801, Alcoy, Spain
[c] Dept. Química Inorgánica e Instituto Universitario de Materiales, Universidad de Alicante, Ap. 99, E-03080, Alicante, Spain

ARTICLE INFO

Keywords:
Perovskite
Spinel
Transition metals
Oxygen reduction reaction
Oxygen evolution reaction
Hydrogen evolution reaction

ABSTRACT

Transition metal oxide-based materials are an interesting alternative to substitute noble-metal based catalyst in energy conversion devices designed for oxygen reduction (ORR), oxygen evolution (OER) and hydrogen evolution reactions (HER). Perovskite (ABO_3) and spinel (AB_2O_4) oxides stand out against other structures due to the possibility of tailoring their chemical composition and, consequently, their properties. Particularly, the electrocatalytic performance of these materials depends on features such as chemical composition, crystal structure, nanostructure, cation substitution level, e_g orbital filling or oxygen vacancies. However, they suffer from low electrical conductivity and surface area, which affects the catalytic response. To mitigate these drawbacks, they have been combined with carbon materials (*e.g.* carbon black, carbon nanotubes, activated carbon, and graphene) that positively influence the overall catalytic activity. This review provides an overview on tunable perovskites (mainly lanthanum-based) and spinels featuring *3d* metal cations such as Mn, Fe, Co, Ni and Cu on octahedral sites, which are known to be active for the electrochemical energy conversion.

1. Introduction

In recent years, society has become increasingly aware of the environmental impact of the use of fossil fuels for energy production. Several international treaties have been reached, especially on global warming due to anthropogenic greenhouse gas emissions and their impact on climate change. The first relevant agreement in this field was the Kyoto protocol, which was achieved in the United Nations Framework Convention on Climate Change in 1997. This set of rules came into force in 2005 and set the objective to reduce the net emissions of greenhouse gases causing global warming (UNFCC, 2008). Another recent treaty was the Paris Agreement, ratified within the United Nations Framework Convention on Climate Change in 2016, where the objective was to keep the global average temperature increase below 2 °C above preindustrial levels and make efforts to limit this increase preferably to 1.5 °C (UNFCC, 2015). Unfortunately, fossil fuels currently dominate the energy market and, in order to achieve the proposed objectives, it is vital to reduce their use and promote renewable energies.

In addition to international agreements, some countries have established their own standards to reduce the use of non-renewable fuels, such as making greater efforts to incorporate renewables into the electric power mix and replacing combustion-engine vehicles with more sustainable electric alternatives (based on either rechargeable batteries or fuel cells). As for combustion engine vehicles, the United Kingdom will ban the sale of this type of car by 2030 (Perry, 2020), while Germany in its action program against climate change foresees that public transport will stop using fossil fuels by 2050 and will forbid the registration of conventional cars in 2035 (Wehrmann, 2020). It is then necessary the development of technologies which, based on alternative energy sources, are able to reduce the emission of greenhouse gases (Mulder et al., 2011; Chel and Kaushik, 2018; Thomas and Zalbowitz, 1999). One of these technologies could be *fuel cells*, which are electrochemical devices that produce electrical energy directly from chemical energy. Fuel cells appeared for the first time in 1839, when William Grove suggested the possibility of producing electricity by electrochemically combining oxygen and hydrogen (Hurley, 2002). Grove called his invention a "gas battery", a device that basically consisted of two platinum electrodes immersed in an electrolyte solution of sulfuric acid and fed with both gases. Since then, fuel cell technology has experienced extensive modifications to improve reagent feed, ion transport, reaction kinetics and, ultimately, its overall efficiency. One of the available technologies is the Alkaline Fuel Cell (AFC) which uses an

* Corresponding author.
E-mail address: morallon@ua.es (E. Morallón).

https://doi.org/10.1016/j.envres.2022.113731
Received 29 March 2022; Received in revised form 14 June 2022; Accepted 16 June 2022
Available online 23 June 2022

alkaline electrolyte such as potassium hydroxide. This technology was developed by NASA in 1960 and, due to its high price and operation characteristics, it is only employed in space missions (Andújar and Segura, 2009). Currently, among the diverse available options, the technology developed in the 1960s by General Electric Co, and known as Proton Exchange Membrane Fuel Cell (PEMFC), seems to be the most promising to replace combustion engines (Andújar and Segura, 2009; Li et al., 2003; Dekel, 2018; Wang et al., 2011).

If the proton exchange membrane is replaced by an anion exchange membrane, we are describing an Alkaline Anion Exchange Membrane Fuel Cell (AAEMFC) (Pan et al., 2018). In the anode of the fuel cell the hydrogen oxidation reaction (HOR) occurs, whereas in the cathode the oxygen reduction reaction (ORR) takes place. Both reactions require a catalyst, which is especially important for the ORR because of its worse kinetics, and current vehicles employing fuel cell technology use Pt-based catalysts for both reactions. Due to the scarcity and high price of this metal, it is very important to develop new catalysts based on alternative elements, which can reduce production costs without reducing their catalytic properties too much (Kongkanand et al., 2019).

The kinetics of ORR is well-known in both acidic and alkaline media. The reaction can proceed mainly through two different routes (Ramaswamy and Mukerjee, 2012; Hong et al., 2015; Shinagawa et al., 2015), as observed in Table 1. The ideal mechanism involves a 4-electron pathway, which produces the direct conversion of O_2 into H_2O or OH^- in acidic and alkaline medium, respectively. This is the preferred route, due to its better energy efficiency and the lack of peroxide formation, which is highly corrosive. However, the reaction can also proceed through a 2-electron pathway, yielding H_2O_2 and HO_2^- in acidic and alkaline medium, respectively. These species can be then reduced to H_2O and OH^-, which results in an overall 2 + 2 electron mechanism. Moreover, both species (H_2O_2 and HO_2^-) can also suffer disproportionation reactions as those described in Eq. 4 in Table 1.

Usually, the more selective catalysts for water formation show higher activity for ORR. In this way, catalysts based on platinum such as platinum nanoparticles supported on carbon materials (Stacy et al., 2017; Wu and Yang, 2013) appear among the best group of catalysts at the moment. They show also some problems such as the lack of stability due to Pt leaching, which is more important in alkaline medium (Zadick et al., 2015), or those derived from the loss of catalytic activity by CO-poisoning, which makes necessary to feed the fuel cell with high purity H_2 (Zhang, 2008).

Multiple strategies have been studied to reduce costs and to improve the stability of Pt-based catalysts. For example, new catalysts were prepared by supporting Pt nanoparticles with different sizes and morphologies on carbon materials (Luo and Alonso-Vante, 2015). However, it is necessary to find cheaper alternatives which, based on more abundant elements, can provide a similar electrocatalytic activity. In this context, metal alloys have been used to enhance some catalytic properties and to lower the price of the final catalyst (Shao et al., 2016). Materials based on transition metal oxides, especially those containing *3d* metals, appeared as suitable alternatives because they gather some key features: their synthesis is usually straightforward, different oxidation states are attainable (which is important for some electrocatalytic applications) and they can be modified to show enhanced electrical conductivity or chemical stability (Hong et al., 2015; Goswami et al., 2018; Osgood et al., 2016). Particularly, metal oxide materials with perovskite or spinel structures are interesting options because it is possible to tailor their chemical structure and composition and, consequently, their physicochemical properties (Goswami et al., 2018; Zhu et al., 2016).

Table 1
Mechanisms proposed in the literature for ORR in acidic and alkaline medium.

Reaction pathways	Acidic medium	Alkaline medium	Eq.
4 electrons	$O_2 + 4H^+ + 4e^- \rightarrow 2H_2O$	$O_2 + 2H_2O + 4e^- \rightarrow 4OH^-$	Eq.1
2 + 2 electrons	$O_2 + 2H^+ + 2e^- \rightarrow H_2O_2$	$O_2 + H_2O + 2e^- \rightarrow HO_2^- + OH^-$	**Eq.**2
	$H_2O_2 + 2H^+ + 2e^- \rightarrow 2H_2O$	$HO_2^- + H_2O + 2e^- \rightarrow 3OH^-$	**Eq.**3
Disprop. Reaction	$2H_2O_2 \leftrightharpoons O_2 + 2H_2$	$2HO_2^- \leftrightharpoons O_2 + 2OH^-$	**Eq.**4

It is worth mentioning that the importance of the oxygen reduction reaction is not limited to PEMFC related technology. Other prominent applications such as metal-air batteries or hydrogen peroxide production make use of such a reaction (Lim and Hoffmann, 2019; Yuan et al., 2011). Contrary to fuel cells, conventional batteries are closed systems where electrode materials play a key role in the redox reactions as "active masses" and energy storage and conversion occur in the same compartment (Winter and Brodd, 2004). On the other hand, metal-air batteries can be considered as hybrid systems, containing a battery electrode in the anode and an electrode fed with oxygen in the cathode. Such an arrangement generates larger energy density because oxygen can be continuously supplied by the atmosphere and no storage is required (Winter and Brodd, 2004; Li and Lu, 2017; Chawla, 2019). Some of these devices are rechargeable, which makes important the oxygen evolution reaction, the reverse reaction to ORR (Shirvanian and van Berkel, 2020; Zhang et al., 2020a; Eftekhari, 2017). Since OER exhibits sluggish kinetics, the use of catalysts based on noble metals, such as RuO_2 or IrO_2 (Ma et al., 2018; Nguyen et al., 2016; Reier et al., 2012), is necessary. Similarly, metal oxide nanoparticles have been employed to reduce costs and to enhance activity (Nguyen et al., 2016) and the stability has been improved by synthesizing alloys with noble metals such as Pt (Ollo et al., 2015). However, it is still necessary to find lower cost alternatives based on more abundant elements. Some transition metal oxides are known to show interesting bifunctional behavior as they can catalyze both ORR and OER (Zhu et al., 2017; Liu et al., 2020a).

OER is closely related to the electrochemical production of hydrogen from water. It is expected that this clean and sustainable energy vector will play a significant role in the near future due to its high specific energy density and unlimited availability (Mazloomi and Gomes, 2012). At present, hydrogen production is based on natural gas reforming and carbon (or biomass) gasification, but water hydrolysis through either photo- or electrolysis has appeared as an eco-friendly promising alternative (Mazloomi and Gomes, 2012; Huang and Wang, 2020; David et al., 2019). Between these two hydrolysis routes, electrolysis seems to be a better option to generate green hydrogen on a large scale. Devices based on Polymer Electrolyte Membrane Electrolyzers (PEME) are attracting great interest for that purpose (David et al., 2019; Abdol Rahim et al., 2016). Such a technology offers some advantages, as those related to the higher purity and outlet pressure of the product, smaller equipment size or higher security level. Apart from those devices based on polymer membrane for alkaline medium (Alkaline Exchange Membrane, AEM) and acidic medium (Proton Exchange Membrane, PEM), alkaline electrolyzers where the electrolyte is a water solution of KOH or solid-state devices (Solid Oxide Electrolysis, SOE) can also be found. Alkaline electrolyzers are preferred for large installations, whereas PEM devices, with better dynamics and gas quality, show better applications in electric energy production for industries or at a residential level. On the other hand, AEM and SOE electrolyzers are technologies still under development and must overcome the stability barriers to compete with other existing technologies (David et al., 2019).

In PEME devices, hydrogen evolution reaction (HER) occurs at the cathode and OER at the anode. Both reactions require a catalyst, although HER is kinetically more favorable. In any case, Pt-based catalysts show probably the best activity for hydrogen formation and the design and optimization of alternative materials is needed (Kemppainen et al., 2015; Xu et al., 2015a). In this review, we will focus on the analysis of metal oxides with either perovskite or spinel structures because they show good electrocatalytic response for this reaction (Zhu et al., 2016; Zhang et al., 2020a; Retuerto et al., 2017). Moreover, transition metal oxides, apart from owning a good response for HER,

also show an outstanding activity for ORR and OER, which make them possible trifunctional catalysts (Zhang et al., 2020b; Wang et al., 2017a). In this context, the bibliographic analysis done will focus only on alkaline media because, on one hand, metal oxides have poor stability in acidic conditions and, on other hand, alkaline electrolytes minimize corrosion problems and the kinetics involved in ORR is slightly more favored. However, polymer alkaline membranes have some limitations due to degradation, making them a technology still under development. Once the aforementioned problems have been solved, AAEMFC batteries can be postulated as a real alternative to replace PEMFC batteries.

2. General description of the electrochemical reaction mechanisms at metal oxides

Diverse factors can influence the electrochemical activity of metal oxides in ORR, OER, and HER. These factors are mostly associated on the one hand to the crystal structure of the compound and, on the other, to the number of available oxygen vacancies. Therefore, before discussing the mechanisms of electrochemical reactions, it is important to analyze the structure of perovskite- and spinel-based metal oxides. The ABO_3 perovskite (Pan and Zhu, 2016; Rao and Meyers, 2003), where A is a rare earth metal or an alkaline earth metal cation and B is a *3d* transition metal cation, shows a cubic structure (Fig. 1a). In this structure, A cations are found at the vertices of the cube and B cations are located in an octahedral environment surrounded by 6 oxygen anions that generate the BO_6 octahedron. According to the crystal field theory (CFT) (Griffith and Orgel, 1957), a *d*-orbital splitting of the B cation generates two orbital groups: a lower energy group of three t_{2g} orbitals and a higher energy group of two e_g orbitals. However, in the presence of vacancies or at the surface, the metal transition orbitals are stabilized adopting a square pyramidal symmetry, where the B cation is surrounded by only 5 oxygen anions. In electrochemical reactions, this configuration favors that reactants and products can interact with the empty position (Grimaud et al., 2013).

BO_6 octahedra can be also found in spinel-based structures, which are cubic close-packed anions arrays where cations are occupying tetrahedral and octahedral environments. In this unit cell of general formula AB_2O_4 (with A and B metals) there are 32 oxygen atoms with 16 cations occupying octahedral sites and 8 cations occupying tetrahedral sites (Fig. 1b) (de Villiers et al., 2003). However, several spinel types can be distinguished (Grimes et al., 1989; Janani et al., 2020): *The normal spinel*, where A cation occupies tetrahedral sites due to its lower crystal field stabilization energy (CFSE), and B cation occupies octahedral sites due to its higher CFSE, which results in the formula $A^{[tet]}B_2^{[oct]}O_4$. In the *inverse spinel*, A cations show higher CFSE and tend to fill octahedral sites, whereas B cations due to its lower CFSE can occupy either octahedral or tetragonal sites, which results in the formula $B^{[tet]}$ $(A^{[oct]}\text{-}B^{[oct]})_2O_4$. *Mixed metal oxide spinels* can also be found (Kaufman, 1993), for which both cations can hold octahedral and tetrahedral sites according to $(A^{II}_{1-x}B^{III}_x)^{[tet]}(A^{II}_xB^{III}_{2-x})^{[oct]}O_4$ stoichiometry, where the inverse spinel is formed for $x = 1$ and a mixed one if $1 > x > 0$.

Generally, octahedral sites show a greater effect than tetrahedral positions on the catalytic activity of the spinel-based structure. This is particularly significant for ORR and OER reactions, for which at octahedral sites the high energy e_g orbital can overlap with the O-containing molecules. On the contrary, at tetrahedral sites neither the e_g nor the t_{2g} orbital point to the oxygen, which leads to a weak interaction with oxygen species (Janani et al., 2020; Liu et al., 2019a). In the following sections, the reaction mechanisms involved in ORR, OER and HER reactions at metal oxides with perovskite- and spinel-based structures will be discussed.

2.1. The oxygen reduction reaction mechanism

The mechanism of the oxygen reduction reaction at metal oxides is governed by the nature of the transition metal involved. Indeed, the optimum interaction between reaction intermediates and the metal site depends strongly on the outer electronic structure of this latter species. For this reason, diverse studies (Sunarso et al., 2012; Ashok et al., 2018; Celorrio et al., 2016a) were carried out to study the influence of the transition metal especially for lanthanum-based perovskites ($LaBO_3$) (see Fig. 2).

Sunarso et al. (2012) investigated this reaction on perovskites substituted with different transition metal cations at the B-site. They reported the following relative electrochemical activity: $LaCoO_3 > LaMnO_3 > LaNiO_3 > LaFeO_3 > LaCrO_3$, a result related with the intrinsic activity of the transition metal. The series of same perovskites was studied by Ashok et al. (2018) who found higher electrocatalytic activity for $LaMnO_3$ as compared to $LaCoO_3$ perovskite. Despite its lower current density, $LaCoO_3$ showed higher stability and was a more feasible option for ORR. Celorrio et al. (2016a) reported also better electrocatalytic activity for $LaMnO_3$, a result that was attributed to the presence of Mn^{3+} species. Particularly, it was suggested that the redox process Mn^{4+}/Mn^{3+} appears close to the oxygen reduction and influences the activity of this perovskite.

Early studies revealed that the electrocatalytic behavior of a transition metal is affected by the number of *d* electrons. In the 80's Bockris and Otagawa (1984) obtained a correlation between this parameter and the strength of Metal-OH^- bonds and Tejuda and Fierro (Tejuca and

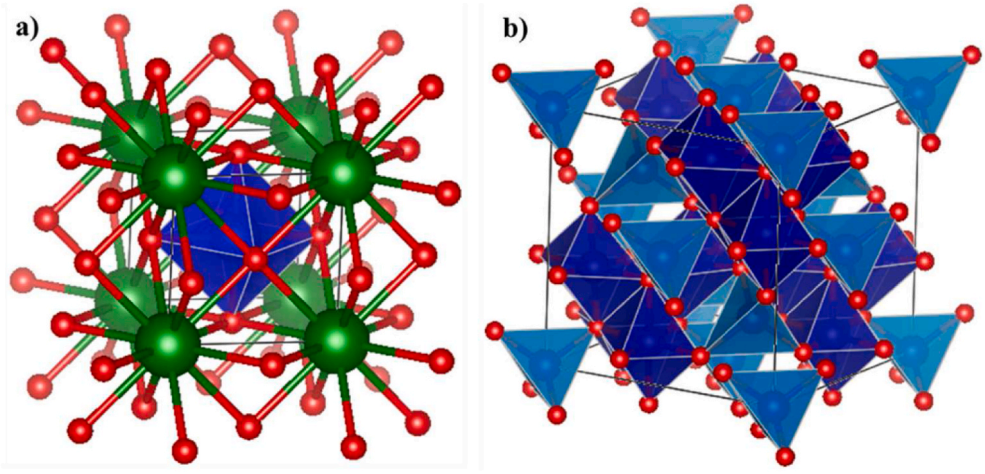

Fig. 1. a) A perovskite-based metal oxide structure where the octahedral site can be observed and **b)** A Spinel-based metal oxide structure where both octahedral and tetrahedral sites can be observed.

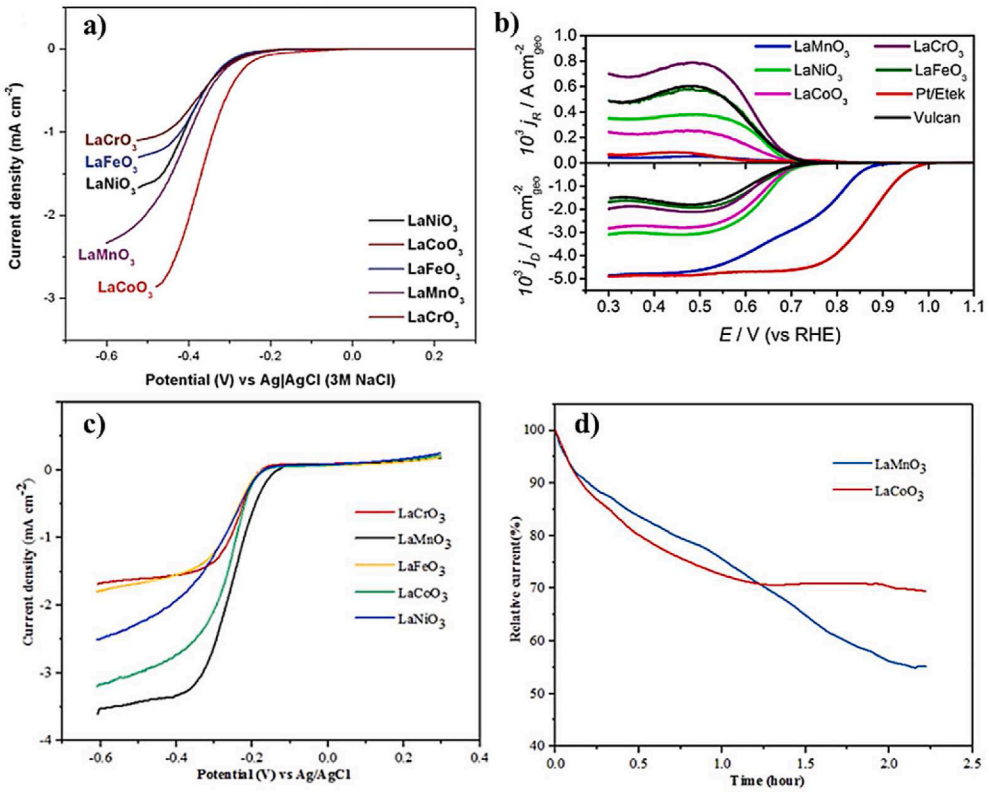

Fig. 2. Study of the catalytic activity of $LaBO_3$ perovskites in ORR **a)** Reprinted with permission from Ref. 59. Copyright 2012, American Chemical Society, **b)** Reprinted with permission from Ref. 61. Copyright 2016, John Wiley and Sons, **c)** Reprinted from Ref. 60. Copyright 2017, with permission from Elsevier, and **d)** Stability of the $LaMnO_3$ and $LaCoO_3$ materials through chronoamperometric experiments. Reprinted from Ref. 60. Copyright 2017, with permission from Elsevier.

Fierro, 1989) reported the metal reactivity for CO oxidation versus the number of *d* electrons in the form of a volcano plot. More recently, Suntivich et al. (2011a) analyzed the effect of e_g orbital filling on the intrinsic activity of transition metals towards ORR by means of the volcano plot, which was adapted by Risch (2017) and it is shown in Fig. 3.

From this plot, it can be concluded that the e_g orbital filling governs the metal-oxygen interaction and an optimum is found when the occupancy of the e_g orbital is close to one electron. In fact, the metal-oxygen species interaction is very strong for fillings below 1 and too weak above this value, which does not benefit the ORR. Fig. 3 reveals that $LaMnO_3$, $LaCoO_3$ and $LaNiO_3$ perovskites are very active materials for this reaction, what is in agreement with the experimental results presented in Fig. 2. Although, there is a disagreement in the order of the specific activity of the oxide materials, which might be related to the physicochemical properties produced by the synthesis method. The importance of e_g orbital filling was implicitly discovered by Matsumoto et al., 1977a, 1977b, who tried to find the factor that governs the catalytic activity of metal oxide perovskites towards ORR. They found that the σ* orbital from the B–OH bond has 1 electron, which comes from the e_g orbital of the transition metal. Moreover, it was demonstrated that the covalency level of the B–O bond between the transition metal and the lattice oxygen influences the rate limiting steps. The mechanism proposed by Suntivich et al. (2011a) and adapted by Li et al. (2016a) is depicted in Fig. 4 and consists of four elementary steps. The rate-determining steps are the OH^-/O_2^{2-} exchange (step 1) and the OH^- regeneration (step 4) on the transition metal surface.

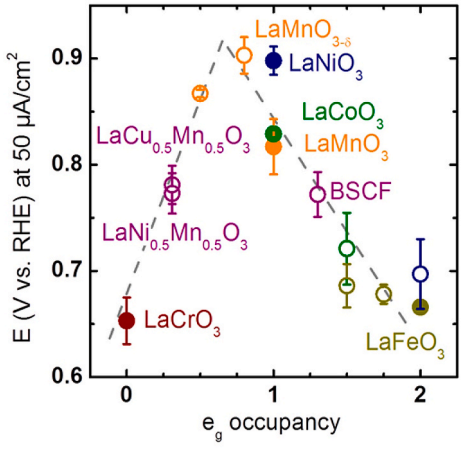

Fig. 3. The relationship between the e_g occupancy and ORR activity of various transition metal oxide surfaces, assessed by the potential at the specific current of 50 μA cm_{ox}^{-2} (current density related to the surface area of oxides). Reprinted from Ref. 65.

In the *first step* an OH^-/O_2^{2-} exchange occurs according to the equation (5).

$$B^{3+} - OH^- + O_2 + \ e^- \rightarrow B^{4+} - BO_2^{2-} + OH^- \quad (5)$$

Firstly, the O_2 molecule interacts with the σ* orbital of the B–OH^- species and then an electron injected from the cathode and an electron from the B cation form the more stable configuration B–O_2^{2-} with the desorption of the OH^- species. As a result, the B^{m+} cation is oxidized to $B^{(m+1)+}$. In the *second step* the reduction of $B^{(m+1)+}$ to B^{m+} occurs and the O_2^{2-} species reacts with a water molecule from the electrolyte to produce a hydroperoxide ion (HO_2^-) and an OH^- is released to the solution. In the *third step,* the adsorbed HO_2^- species reduces to yield adsorbed O^{2-} and OH^- (released to the solution) because two electrons are again gained from the cathode and the metal producing the oxidation of B^{m+} to $B^{(m+1)+}$. Finally, in the *fourth step*, O^{2-} adsorbed on the

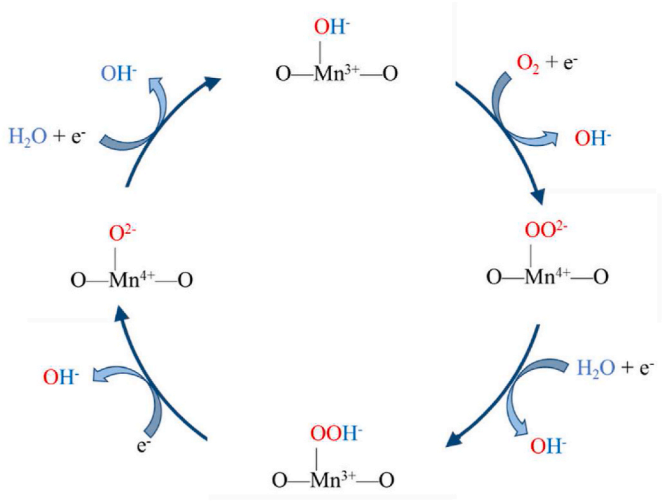

Fig. 4. Proposed mechanism for perovskite-based materials in ORR. Adapted from Li et al. Reprinted from Ref. 68. Copyright 2016, with permission from Elsevier.

cation combines with a water molecule to yield two OH^- ions; one is released to the solution and the other remains adsorbed on B^{m+}, which was obtained from the reduction of $B^{(m+1)+}$ by the cathodic current. The rate-determining step depends on the occupancy of e_g orbitals: above 1 electron, the OH^-/O_2^{2-} exchange is slowed because it is not formed a more stable interaction between the exchanged specie and the B-site cation during the displacement, thus the ORR reaction kinetics may be limited by the rate of OH^-/O_2^{2-} exchange (step 1). However, for an occupancy below 1 electron, the B–O^{2-} species is not sufficiently destabilized and the reaction is limited by OH^- regeneration (step 4) (Suntivich et al., 2011a). The same mechanism can be applied to spinel-based materials (Lee et al., 2015a; Wang et al., 2018) because *3d* transition metals are also in an octahedral site in this structure. Long et al. (2019) confirmed that the catalytic activity to ORR depends on the covalency of the B–O bond (oxygen from the lattice) by using soft X-ray Absorption Spectroscopy (sXAS).

Several studies revealed the role played by oxygen vacancies in ORR (Risch, 2017; Ji et al., 2020; Matsumoto et al., 1978). Matsumoto et al. (1978) studied their effect in $LaNiO_3$ perovskite and found that HO_2^- species adsorbed on the transition metal cation can combine with Ni^{3+} active sites and oxygen vacancies making the reduction to OH^- easier. Fig. 5 shows the reaction mechanism involving oxygen vacancies as interpreted by Risch (2017). The active site is depicted as two transition metal atoms with OH^- adsorbed and an oxygen vacancy (c1). Then, an OH^- ion is displaced by an O_2 molecule which interacts with a metal site and occupies the oxygen vacancy (c2). In the next step (c3) a water molecule interacts with the adsorbed dioxygen producing the breaking of the O–O bond, thus releasing an OH^- and leaving an O species in the vacancy position. Then, a further interaction with a water molecule occurs producing an OH^-, which is released to the solution, and a H^+ species that interacts with O in the oxygen vacancy position yielding and OH species. Finally, the oxygen vacancy is recovered through the release of OH^-. In each one of these four steps an electron is supplied by the cathode giving rise to the four electron reduction of the dioxygen molecule.

The mechanisms described above involve a 4-electron pathway. However, in an alkaline medium the oxygen reduction reaction can also proceed through a 2 + 2 electron pathway or, alternatively, through a chemical reduction (Mattick et al., 2018; Miyahara et al., 2014). The detailed mechanisms are described in Table 1 for alkaline medium. At low overpotentials (roughly between 0.5 and 0.7 V) the reduction proceeds through either a 4-electron pathway (Eq. 1) or a 2-electron pathway generating HO_2^- (Eq. 2). The peroxide species cannot be

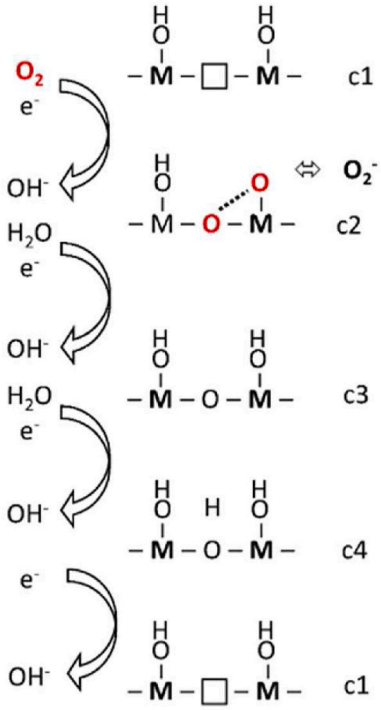

Fig. 5. Mechanism for ORR involving the lattice oxygen vacancies from the metal oxides. The square represents an oxygen vacancy. Reprinted from Ref. 65.

subsequently reduced to OH^- at such a high potential and, instead, it undergoes a disproportionation reaction (Eq. 4). In contrast, at higher overpotentials (~0.25 V), peroxide ions are reduced electrochemically to yield hydroxyl ions through a 2-electron pathway (Eq. 3).

2.2. The oxygen evolution reaction mechanism

The mechanism for the oxygen evolution reaction on perovskite and spinel-based metal oxide materials also involves *3d* metal cations as active sites, which are in octahedral environment. The presence of oxygen vacancies in metal oxide centers also improves the electrocatalytic activity through OER.

The OER mechanism at metal oxide perovskites was established in the studies of Bockris and Otagawa (1984). It was concluded that the rate-determining step in OER is the reaction of OH^- with the adsorbed O_2^- to generate adsorbed HO_2^-. In parallel to ORR, filling with 1 electron the σ* orbital of the B–OH^- bond (coming from 1 electron in the e_g orbital of the transition metal) also seems to be important due to the participation of these species in the reaction mechanism. In this sense, the strength of the B–OH^- interaction has a strong influence in the reaction mechanism, where moderate values are preferred to maximize the performance of the reaction and to generate the desired product, according to the Sabatier's principle (Medford et al., 2015). Suntivich et al. (2011b), who studied both OER and ORR, reported a volcano plot connecting the e_g orbital filling with the measured potential at a constant current density. The optimum filling was suggested to be of ~1.2 electrons (Fig. 6). A high covalency of B–O bonds is also relevant because it promotes the charge transfer between surface cations and adsorbed species such as O_2^{2-} and O^{2-}, which results in a higher activity of OER. From the results in Fig. 6, it is concluded that $LaCoO_3$ and $LaNiO_3$ are the most active perovskites of the $LaBO_3$ series.

Among the reaction mechanisms proposed for OER, the *adsorbate evolution reaction mechanism* (AEM) considers that the redox processes of the transition metal are essential for the development of the reaction. OER progresses in the opposite direction to ORR, as it can be observed in Fig. 7a (Suntivich et al., 2011b; Mefford et al., 2016; Rong et al., 2016;

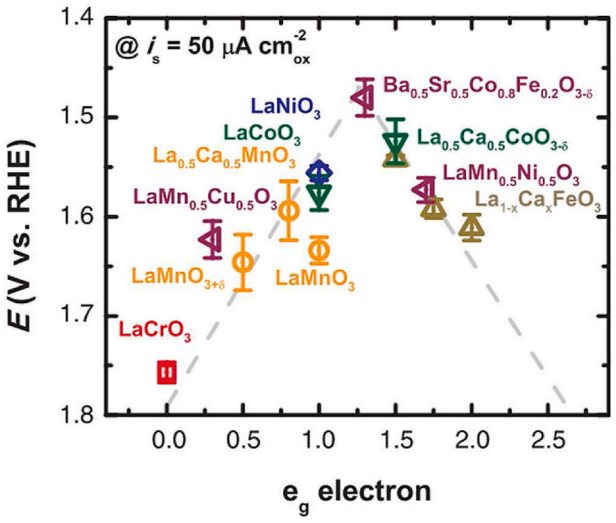

Fig. 6. The relationship between e_g occupancy and OER activity at perovskite-based metal oxide materials, assessed by the potential at the specific current of 50 μA cm^{-2}_{ox} (current density related to the surface area of oxides). From Ref. 77. Reprinted with permission from AAAS.

Yoo et al., 2018), with two rate-determining steps: the formation of an O–O bond in HO_2^- adsorbed on a B cation (step 2) and the deprotonation of HO_2^- to generate O_2^{2-} (step 3). The *first step* starts with OH^- adsorbed on a B^{m+} cation that reacts with another OH^- species to generate H_2O and O_2^-. Also, an electron is generated as a result of the oxidation of B^{m+} to $B^{(m+1)+}$. In the *second step*, O_2^- species adsorbed on $B^{(m+1)+}$ reacts with OH^- to yield HO_2^-, thus reducing the metal cation to B^{m+} and releasing 1 electron. In the *third step*, an OH^- species coming from the solution interacts with HO_2^- to give H_2O and O_2^{2-}, which remains adsorbed on the cation and is able to oxidize the metal species to $B^{(m+1)+}$. Finally, in the *fourth step*, the O_2^{2-} species adsorbed on a $B^{(m+1)+}$ cation is replaced by OH^-, which produces O_2, the release of one electron and the recovery of B^{m+} oxidation state.

On the other hand, Fig. 7b shows the mechanism that considers the covalency of the B–O bond and the role played by oxygen vacancies. Such a mechanism is known as the *lattice oxygen oxidation mechanism* (LOM) (Mefford et al., 2016; Rong et al., 2016; Yoo et al., 2018). The *first step* starts with an adsorbed OH^- species on the B^{m+} cation that reacts with OH^- from the solution, yielding H_2O and releasing 1 electron. Besides, a surface O transfer generates O_2^- species and the O vacancy. In a *second step*, an exchange of O_2^- species with OH^- in solution takes place to generate O_2 and 1 electron. In the *third step*, the O vacancy becomes unstable and OH^- fills the vacancy and protonates the surface O lattice, which generates 1 electron. Finally, in the *fourth step*, OH^- from the solution reacts again to yield H_2O and 1 electron and inducing a deprotonation that restores the initial surface. In the case that the material owns surface O vacancies, the LOM mechanism occurs from the third step (Rong et al., 2016). It is worth mentioning that there exists a direct relation between the covalency of the B–O bond and the presence of oxygen vacancies, because the latter can increase the overlapping of M *3d* and O *2p* orbitals, thus enhancing the covalency of the bond, which favors OER (Mefford et al., 2016).

These two mechanisms can occur at metal oxide-based materials, but from a global energy point of view, the LOM mechanism is slightly more favorable than AEM mechanism (Yoo et al., 2018), which demonstrates the significant role of lattice oxygen and oxygen vacancies. It is worth noting that a high concentration of oxygen vacancies could be detrimental, since the metal oxide stability decreases due to cation leaching and the surface structure can be damaged (Rong et al., 2016). Similarly to ORR, the OER reaction can proceed through two different reaction mechanisms (Mattick et al., 2018; Miyahara et al., 2014) involving the equations described previously in Table 1 for alkaline conditions (Eq. 1-Eq. 4) but in the opposite direction. O_2 can be produced through a 4-electron pathway (Eq. 1) but also by a 2 + 2 electron pathway. At low potentials, HO_2^- is generated through a 2-electron pathway (Eq. 3), followed by oxidation to O_2 by a further 2-electron pathway (Eq. 2). At high potentials, HO_2^- is obtained again (Eq. 3) and it is subsequently oxidized to O_2 through a disproportionation reaction (Eq. 4).

2.3. Hydrogen evolution reaction mechanism

The hydrogen evolution reaction proceeds in an alkaline medium through either a combination of Volmer-Tafel or Volmer-Heyrovsky mechanisms (Wei et al., 2018; Sheng et al., 2013; Pennycook et al., 2014), which are summarized in Table 2. Both of them involve the adsorption of a H_2O molecule on the metal surface and its subsequent electrochemical reduction to OH^- together with the formation of H_{ads} as an intermediate species.

The first volcano plot in an acidic medium was reported by Trasatti (1972). The exchange current density, which is related with the equilibrium reaction, was represented versus the metal hydride (M-H) energy of formation. Sheng et al. (2013) performed similar studies in

Table 2
Mechanisms involved in the hydrogen evolution reactions.

Volmer-Tafel	Volmer-Heyrovsky
$H_2O + e^- \rightarrow H_{ads} + OH^-$	$H_2O + e^- \rightarrow H_{ads} + OH^-$
$H_{ads} + H_{ads} \rightarrow H_2$	$H_{ads} + H_2O + e^- \rightarrow H_2 + OH^-$

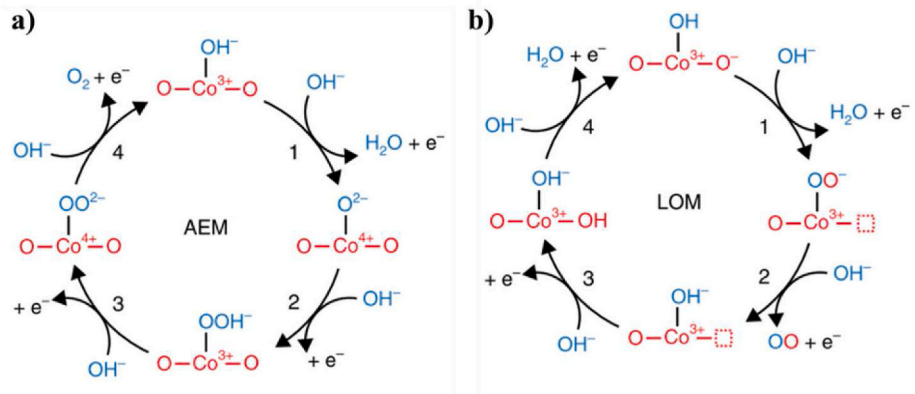

Fig. 7. Mechanisms involved in OER: **a)** AEM and **b)** LOM. The squares represent oxygen vacancies. Reprinted from Ref. 78.

alkaline medium and found a relation between the exchange current density and the hydrogen adsorption energy. The reaction rate in HER also depends on the strength of the M-H_{ads} interaction and, according to the Sabatier principle, it is preferable a moderate interaction to promote the formation of H_2. From the plot it was concluded that Ni, Co, and Fe exhibit better activity towards HER. Meanwhile, Quaino et al. (2014) related the activity of metals in HER to the free energy for H adsorption and found a better electrocatalytic response for Ni and Co.

3. Perovskite metal oxide-based catalysts

As mentioned above, perovskite metal oxide-based materials with $LaBO_3$ structure are of great interest for electrocatalytic reactions involving molecular oxygen. The wide use of lanthanum as the A-cation is based on the results obtained after the substitution of a set of lanthanides in the $AMnO_3$ structure. It was observed that the catalytic activity decreases in the order: La > Pr > Nd > Sm > Gd > Y > Dy > Yb (Hyodo et al., 1996). La^{3+}, having no 4f electrons, provides better electrical conductivity and, consequently, an enhancement of the electrocatalytic activity (Kozuka et al., 2015). In contrast, the decrease in the ionic radius in the previous series of elements produces a reduction of the Goldschmidt tolerance factor, which results in the formation of progressively less symmetrical structures, which induce distortion and rotation of the BO_6 octahedron. Among those cations without 4f electrons, La^{3+} offers better results compared to, for example, Y^{3+} (Kozuka et al., 2015) mainly because of a better compromise between ionic radius and 4f electrons is reached. Celorrio et al. (2018) studied the effect of substituting the A-cation in $AMnO_3$ perovskites (A = Y, Ca, La, Sr) and reported that $LaMnO_3$ was the best material under ORR conditions. This was attributed to the formation of an octahedral site around the Mn^{3+} cation, with very similar Mn–O bond distances. In contrast, for $YMnO_3$ and $SrMnO_3$ different Mn–O bond distances were observed, which cannot provide the ideal octahedral site for the catalytic activity.

Despite that some studies (Li et al., 2016a; Kim et al., 2016; Li et al., 2018; Kéranguéven et at., 2017; Miao et al., 2020) pointed to the existence of a certain bifunctional character of $LaMnO_3$ towards ORR and OER, this material showed poor long-term stability. In this way, more stable metal oxide perovskites such as $LaCoO_3$ (Ashok et al., 2018; Liu et al., 2017; Yang et al., 2018) and $LaNiO_3$ (Lee et al., 2015b; Alexander et al., 2018) were suggested for both reactions. However, metal oxide perovskite materials with La in their structure tend to be almost inactive towards HER. The only exception appears when different A-cations are combined, as in $La_{0.5}(Ba_{0.4}Sr_{0.4}Ca_{0.2})_{0.5}Co_{0.8}Fe_{0.2}O_{3-\delta}$. This material supported on reduced graphene oxide (rGO) has a structure quite similar to the $LaBO_3$-based structure previously described, which shows a bifunctional character for OER and HER (Hua et al., 2017).

3.1. Perovskite metal oxide-based materials with partial substitution of A-site cation

The use of lanthanum at A-sites in $LaBO_3$ perovskites (where B is a 3 d transition metal) provides these metal oxides with better catalytic activity for a number of reactions. However, the catalytic activity can be significantly improved after a partial substitution of A cations with lower valence elements, such as alkaline-earth metals. This generates on the one hand more oxygen vacancies and, on the other, an increase of the ratio B^{4+}/B^{3+} to compensate charges. It was observed that these two effects improve the catalytic activity in electrochemical reactions (Chen et al., 2015).

Strontium is one of the most studied alkaline-earth metals to partially substitute La^{3+} as the A-cation in metal oxide perovskites: $La_{1-x}Sr_xMnO_3$ (Chen et al., 2017; Yuan et al., 2019a; Xue et al., 2017; Zhao et al., 2017a; Stoerzinger et al., 2015) and $La_{1-x}Sr_xCoO_3$ (Mefford et al., 2016, 2019). A suitable ORR performance was observed for the former group of materials when Sr concentration was around 30% (Xue et al., 2017; Stoerzinger et al., 2015). Such a value seems to favor an optimum Mn^{4+} concentration that generates oxygen vacancies and increases the electrical conductivity. On the other hand, the covalency of the Mn–O bond is enhanced, which favors the electron transfer and the adsorption of oxygen on the perovskite. In the case of $La_{0.8}Sr_{0.2}MnO_3$, good results were obtained for both ORR and OER (Chen et al., 2017; Yuan et al., 2019a). Yuan et al. (2019a) studied the possibility of generating more oxygen vacancies by means of the A cation deficiency, which favors the catalytic activity of the material because the kinetics is improved. Zhao et al. (2017a) reported good catalytic activity for ORR and OER with a $La_{0.4}Sr_{0.6}MnO_3$ perovskite. Again, the best performance was attributed to a combination of factors: the formation of a Mn^{3+}/Mn^{4+} redox couple, a higher covalency of the M-O bond and a larger Mn^{4+} concentration. Mefford et al. (2019) reported 40–60% as the optimum Sr concentration for this type of metal oxide perovskite for a good catalytic performance in ORR. In the case of OER, the oxide $SrCoO_{2.7}$ (Mefford et al., 2016) exhibited better catalytic activity because of its higher concentration of oxygen vacancies, which actively participate in the reaction mechanism.

Apart from strontium, another alkaline-earth metal employed in some works to substitute lanthanum is Ca^{2+} (Celorrio et al., 2016b; Bradley et al., 2019; Abe et al., 2020). Celorrio et al. (2016b) reported a progressive reduction of activity of these materials towards ORR on increasing Ca concentration and, unfortunately, the most active perovskite was the unsubstituted one. The change in activity compared to the pure lanthanum perovskite can be ascribed to diverse factors, such as the formation of less symmetrical structures or the greater tendency of La^{3+} to segregate at the metal oxide surface with respect to Ca^{2+}, which somehow promotes the optimum oxidation state of Mn. Abe et al. (2020) observed that, in a $La_{1-x}Ca_xNiO_3$ perovskite series, the incorporation of calcium decreased the e_g orbital filling below 1 electron, which worsened its catalytic activity towards ORR.

3.2. Perovskite metal oxide-based materials with partial substitution of B-site cation

To enhance the catalytic activity and stability of $LaBO_3$ materials under ORR and OER conditions, a partial substitution of B cations has been studied. Such a process usually results in the appearance of different effects such as synergy between the two cations, beneficial morphological modifications or better reaction kinetics induced by the presence of mixed oxidation states (Chen et al., 2015). Sunarso et al. (2012) studied the effect of replacing 50% of Ni cations in $LaNiO_3$ perovskites with other *3d* transition metals. They reported a larger current density for ORR that decreases in the order $LaNi_{0.5}Mn_{0.5}O_3$ > $LaNi_{0.5}Cr_{0.5}O_3$ > $LaNi_{0.5}Co_{0.5}O_3$ > $LaNi_{0.5}Fe_{0.5}O_3$ > $LaNiO_3$. The enhancement observed in the catalytic performance was attributed to the appearance of a synergistic effect between both cations that favors the reaction kinetics.

Due to the good catalytic activity of $LaMnO_3$ and $LaCoO_3$, several authors proposed doping $LaMnO_3$ perovskites with cobalt (Hu et al., 2015; Lee et al., 2015c; Liu et al., 2018; Lv et al., 2019; Sun et al., 2020; Vazhayil et al., 2022). Particularly, Hu et al. (2015) and Lee et al. (2015c) observed that a small cobalt substitution is sufficient to produce a significant improvement of the catalytic response in ORR, with a better onset potential and a higher current density. Moreover, the incorporation of Co to $LaMnO_3$ induces the formation of oxygen vacancies that facilitate oxygen diffusion, increase the electrical conductivity of the material and favor the oxygen adsorption. Another effect caused by this substitution is the occurrence of Mn^{3+}/Mn^{4+} and Co^{2+}/Co^{3+} redox pairs that enhance the electrical conductivity and, in addition, the increase of Mn^{4+}concentration offers a higher oxidation capacity than Mn^{3+}. It was also concluded that the presence of Co favors the filling of the e_g orbital until an optimum value to enhance catalytic activity. Instead, Liu et al. (2018) reported small differences in ORR and found that $LaMnO_3$ exhibits the best catalytic response because the presence of Co induced undesired changes in the crystal structure. On the contrary, under OER conditions $LaMn_{0.7}Co_{0.3}O_3$ material shows the best performance,

making it a suitable alternative for bifunctional catalysts. On the other hand, Lv et al. (2019) made a small substitution of Cu and Co in $LaMnO_3$ perovskites and reported high catalytic activity towards both reactions (Fig. 8a and b) and good stability that was associated to the occurrence of higher Mn^{4+} concentration that compensates the presence of a lower-valence cation. The high oxidation state of manganese benefits the O_2^-/OH^- exchange and favors the disproportionation reaction of HO_2^- to O_2. In addition, oxygen vacancies are generated, what increase the covalency of the B–O bond and also favors the O_2^-/OH^- exchange, thus improving the activity for ORR. Sun et al. (2020) reported in a similar study the doping of $LaCoO_3$ perovskite with Mn. They concluded that the best bifunctional material for ORR and OER was $LaMn_{0.3}Co_{0.7}O_3$ (Fig. 8c and d). The enhancement was associated to the filling of e_g orbital with* approximately 1 electron (value closer to the optimum value of 1 electron compared to 1.23 estimated for the $LaCoO_3$ sample). In addition, the covalency of the Co–O bond was improved, which promoted the reaction kinetics. In the same way, Vazhayil el at (Vazhayil et al., 2022). reported that the $LaMn_{0.2}Co_{0.8}O_3$ perovskite had a good stability and acceptable OER activity. The good performance was associated to the mesoporous structure and to the presence of Co^{3+} and Mn^{4+} ions on the surface, which enhance OER activity. Moreover, the introduction of Co improves the charge transfer and promotes an e_g orbital filling close to the unity (~0.97), which are beneficial for OER.

Flores-Lasluisa et al., 2019a, 2020a studied the $LaMnO_3$ perovskite modified to include cobalt centers in B sites formerly occupied by Mn. Lanthanum ions are always predominant at the surface of the $LaMn_{1-x}Co_xO_3$ catalyst but high cobalt-substitution levels stimulate the surface enrichment in B cations in their respective higher oxidation states (Mn^{4+} and Co^{3+} against Mn^{3+} and Co^{2+}). The presence of cobalt at low concentration influences the catalytic activity positively, and better bifunctionality is attained. However, their low electrical conductivity limits their applicability in electrochemical devices and the electrochemical performance improved significantly by physically mixing with carbon black. The existence of a synergistic effect between the metal oxide perovskite and the carbon material was interpreted in the light of a strong carbon–oxygen–metal interaction, obtaining promising electrocatalysts towards both ORR and OER.

In the search for the best bifunctional catalyst for ORR and OER, other authors have chosen the combination of Co^{2+} and Ni^{2+} cations in B positions. This strategy is based on the contrasted catalytic power of Ni under OER conditions. The partial substitution of Ni in $LaCoO_3$ perovskite has also a positive effect on ORR due to the formation of a Ni^{3+}/Ni^{2+} redox couple and oxygen vacancies, which enhance not only the electrical conductivity, but also and the catalytic activity (Vignesh et al., 2016; Kalubarme et al., 2014; Wang et al., 2019). Vignesh et al. (2016) observed a positive effect in OER caused by the replacement of Ni by Co in $LaCo_{0.97}O_{3-\delta}$, as well as a significant improvement of stability. The incorporation of Ni to octahedral centers increases the number of catalytic sites and affects the e_g orbital filling, thus decreasing the adsorption strength of OH^- species and improving the OER performance. Wang et al. (2019) concluded that $LaCo_{0.5}Ni_{0.5}O_3$ exhibits good stability under potential cycling and it can be employed as a bifunctional catalyst for ORR and OER.

Apart from binary combinations, more complex assortments implying Mn^{3+}, Co^{2+} and Ni^{2+} cations have been studied. Sun et al. (2021) synthesized $LaMnNiCoO_3$ perovskites (with 1:2:3 ratio for Mn: Ni:Co) and reported higher catalytic activity than $LaCoO_3$ for ORR and OER, which was attributed to the filling of e_g orbital with almost 1 electron and to the better kinetics resulting from the higher covalency of the Co–O bond. Bradley et al. (2019) studied the effect of replacing Mn by Ni and found good catalytic behavior of $La_{0.85}Mn_{0.7}Ni_{0.45}O_{3-\delta}$ material in both reactions, which was ascribed to diverse factors, such as the presence of oxygen vacancies created by the substitution of Ni^{2+} by La^{3+}, the formation of Mn^{3+}/Mn^{4+} and Ni^{2+}/Ni^{3+} redox couples and the

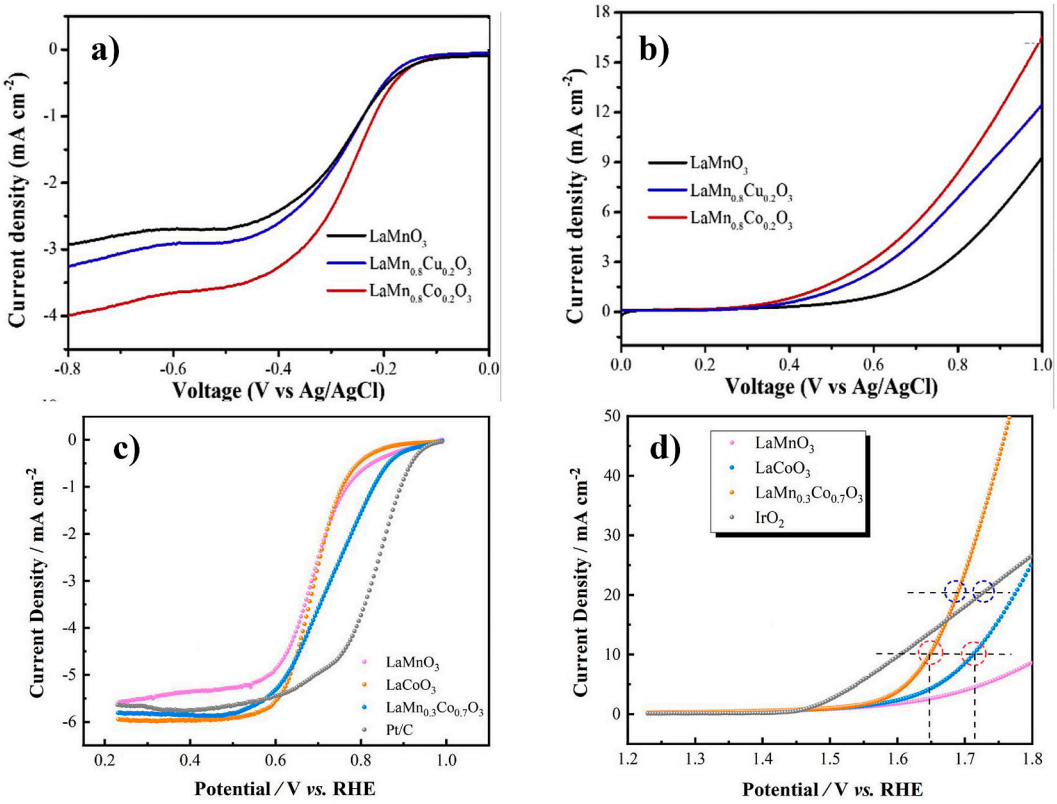

Fig. 8. a) and **b)** Catalytic activity of $LaMnO_3$ and $LaMn_{0.8}B_{0.2}O_3$ materials (B= Cu and Co) in ORR and OER, respectively. Reprinted from Ref. 111. Copyright 2019, with permission from Elsevier. **c)** and **d)** Catalytic activity of $LaMnO_3$, $LaCoO_3$, and $LaMn_{0.3}Co_{0.7}O_3$ materials in ORR and OER, respectively. Reprinted with permission from Ref. 112. Copyright 2020, American Chemical Society.

increase of Mn^{4+} concentration, which favors the disproportionation reaction.

3.3. Perovskite metal oxide-based materials with partial substitution of A and B cations

Some studies have shown that the simultaneous and partial substitution of A and B cations may have a positive influence on the catalytic activity of metal oxide perovskites towards ORR and OER. Due to the improved activity observed after partial replacement of Sr by La, great attention was paid to the substitution of B centers in $La_{1-x}Sr_xB_{1-x}B'_xO_3$ materials, where B and B′ were *3d* transition metals (Yuan et al., 2019a; Park et al., 2015; Majee et al., 2018; Safakas et al., 2019; Alegre et al., 2018; Wang et al., 2016a; Zhao et al., 2018; Aoki et al., 2018). Among the diverse combinations of *3d* transition metals, probably the most studied involves Fe and Co, despite the presence of iron was reported to decrease the number of oxygen vacancies and to increase the filling of e_g orbitals (Safakas et al., 2019). This makes the interactions between oxygen species and B cations stronger and increases the risk of obtaining a limited ORR activity. Majee et al. (2018) observed that nanoparticles of $La_{0.699}Sr_{0.301}Co_{0.702}Fe_{0.298}O_{3-\delta}$ ($\delta = 0.05–0.11$) exhibit the best electrocatalytic response in OER, which was attributed to their crystal structure and to the fact that this composition favors OH^- adsorption and O_2 desorption, which enhance the reaction kinetics. The presence of cobalt favors ORR and iron favors OER, which makes materials based on the formula $La_{1-x}Sr_xCo_{1-x}Fe_xO_3$ suitable as bifunctional catalysts (Park et al., 2015; Alegre et al., 2018).

The positive effect of introducing Fe was also studied in $La_{0.8}Sr_{0.2}MnO_3$ by replacing half of Mn sites. A better catalytic behavior was observed, especially for OER, due to the higher concentration of oxygen vacancies that improves reaction kinetics (Yuan et al., 2019a). Other researchers studied the effect of introducing Ni in $La_{1-x}Sr_xMnO_3$ perovskites (Wang et al., 2016a; Aoki et al., 2018). Aoki et al. (2018) observed that replacing 10% Mn by Ni is sufficient to obtain a good catalytic activity in ORR due to the presence of 1 electron in the e_g orbitals, which resulted from the higher concentration of Mn^{3+} on the surface. However, Wang et al. (2016a) replaced a higher proportion of Mn and reported better bifunctional character for the resulting $La_{0.8}Sr_{0.2}Mn_{0.6}Ni_{0.4}O_3$ perovskite. The additional redox pair, that increases the specific surface area and the number of oxygen vacancies, was suggested to be at the origin of the improvement. In fact, high Mn^{4+} concentration is one of the factors that can enhance the activity towards ORR, whereas high Ni^{3+} concentration could favor OER. Zhao et al. (2018) carried out a similar study, but they replaced Mn by Co and observed enhanced bifunctionality for $La_{0.8}Sr_{0.2}Mn_{0.6}Co_{0.4}O_3$, which was attributed to the presence of oxygen vacancies and higher Mn^{4+} concentration that favor both reactions. However, in this case OER was not promoted, which was explained in terms of the lower catalytic activity of Co^{3+} compared to Ni^{3+}.

4. Spinel metal oxide-based catalysts

The spinel-based structure can be formed with a single *3d* transition metal. In this case, the formula is expressed as M_3O_4, where M is usually Mn, Fe or Co. Among these materials, Mn_3O_4 and Co_3O_4 show a standard spinel structure where M^{3+} cations occupy octahedral sites, whereas Mn^{2+} cations are located in tetrahedral sites with a 2:1 ratio (Chai et al., 2017; Reddy et al., 2017). The structure of Fe_3O_4 is that of an inverse spinel, where Fe^{2+} cations are located in a half of octahedral sites and Fe^{3+} cations occupy both sites (Rado et al., 2017).

Materials with Mn_3O_4 structure have been investigated mainly for ORR due to the good catalytic activity of Mn^{3+} species in the octahedral position (Chai et al., 2017; Najam et al., 2020; Wu et al., 2019; Gao and Geng, 2014; Liu et al., 2016a; Zhang et al., 2020c). Many of these studies focused on the support employed because it can enhance the catalytic activity of the metal oxide. For example, reduced graphene oxide (rGO) was reported to improve the electrical conductivity of the metal oxide (Chai et al., 2017). Other suitable supports are N-doped carbon materials, which provide high electrical conductivity (Najam et al., 2020; Wu et al., 2019; Gao and Geng, 2014). In addition, a synergistic effect between the constituting materials seemed to improve the catalytic activity through formation of Mn–N–C bonds. Those interactions favor the electron transfer (Wu et al., 2019) and the presence of N species lowers the adsorption energy of O_2 (Najam et al., 2020). Liu et al. (2016a) synthesized Mn_3O_4 with different morphology and obtained nanoflake-like structures whose (001) plane are more active than (101) plane, because the first electron transfer process is thermodynamically more favored in this (001) plane. Another interesting way of increasing the ORR activity consists on generating Mn defects that improve the electrical conductivity and increase the surface Mn^{3+} concentration (Zhang et al., 2020c).

The iron Fe_3O_4 spinel has been applied mainly to ORR, despite it shows certain activity towards OER and HER. To improve its catalytic activity, the metal oxide has been supported on carbon materials with better electrical conductivity and higher surface area, such as reduced graphene oxide (rGO) (He et al., 2021) and porous N-doped carbon materials (Zhang et al., 2019; Li et al., 2016b; Hu et al., 2020; Deng et al., 2020). Apart from high surface area, the latter presents several advantages related to N sites, such as pyridinic and graphitic sites, which enhance the adsorption of O_2 and to the formation of Fe–N–C bonds that enhance ORR. Hu et al. (2020) encapsulated Fe_3O_4 nanoparticles in a carbon support with micro- and macroporosity. The microporosity favored the formation of Fe_3O_4 nanoparticles in the cavities. Moreover, the carbon material also contains atomically dispersed Fe–N–C species which can be active for ORR. The combination of both elements favored the O_2 adsorption on Fe–N–C, which increased the activity towards ORR. Deng et al. (2020) observed the formation of oxygen vacancies in the Fe_3O_4 spinel when supported on an N-doped mesoporous carbon material, what favor the ORR kinetics.

Some studies have demonstrated that Fe_3O_4 can be also employed as electrocatalyst for OER (Wei et al., 2020; Zhang et al., 2020d). Wei et al. (2020) studied the effect of synthesis temperature on this metal oxide spinel and observed that calcination at 450 °C generates porous structures that generate high surface area and structural defects that favor the OER kinetics. Zhang et al. (2020d) tried to increase the OER activity of Fe_3O_4 by an in situ electro-reduction method that generated a rougher surface structure, a reduction of the Fe^{3+}/Fe^{2+} ratio, and an increase in the concentration of surface OH^-. All these factors seem to increase the ORR activity. On the other hand, Liu et al. (2019b) obtained a multifunctional catalyst by synthesizing Fe_3O_4 nanoparticles from an ionic liquid that contained Fe. The nanoparticles were then supported on an N-doped porous carbon material obtained from biomass. The good catalytic response for OER and HER (Fig. 9a, b, c) was associated to the presence of N functional groups, which improve the electrical conductivity of the carbon material and facilitates the adsorption of OH^- and H* species. N functional groups and metal oxide nanoparticles enhance the electrocatalytic activity in ORR by a synergistic effect.

Hybrid materials formed by carbon materials and Co_3O_4 spinel showed a promising catalytic behavior for both ORR (Liang et al., 2011; Wang et al., 2013; Liu et al., 2020b) and OER (Xu et al., 2016; Yao et al., 2016; Leng et al., 2017). For this reason, diverse studies focused on the development of bifunctional catalysts with optimized performance for both reactions (Wang et al., 2017b; Zhao et al., 2017b; Jia et al., 2017, 2019; Su et al., 2019; Guo et al., 2019; Tomon et al., 2021). N-doped carbon materials were used in most of these works (Wang et al., 2017b; Jia et al., 2017, 2019; Guo et al., 2019) because they offer specific active sites that improve the ORR avoiding the agglomeration of metal oxide nanoparticles. Moreover, a strong synergy between N functional groups and Co_3O_4 was observed. That effect improves considerably the electron transfer and hence the catalytic activity (Wang et al., 2017b; Guo et al., 2019). Su et al. (2019) and Tomon et al. (2021) focused their efforts in enhancing the electrical conductivity and the catalytic activity by

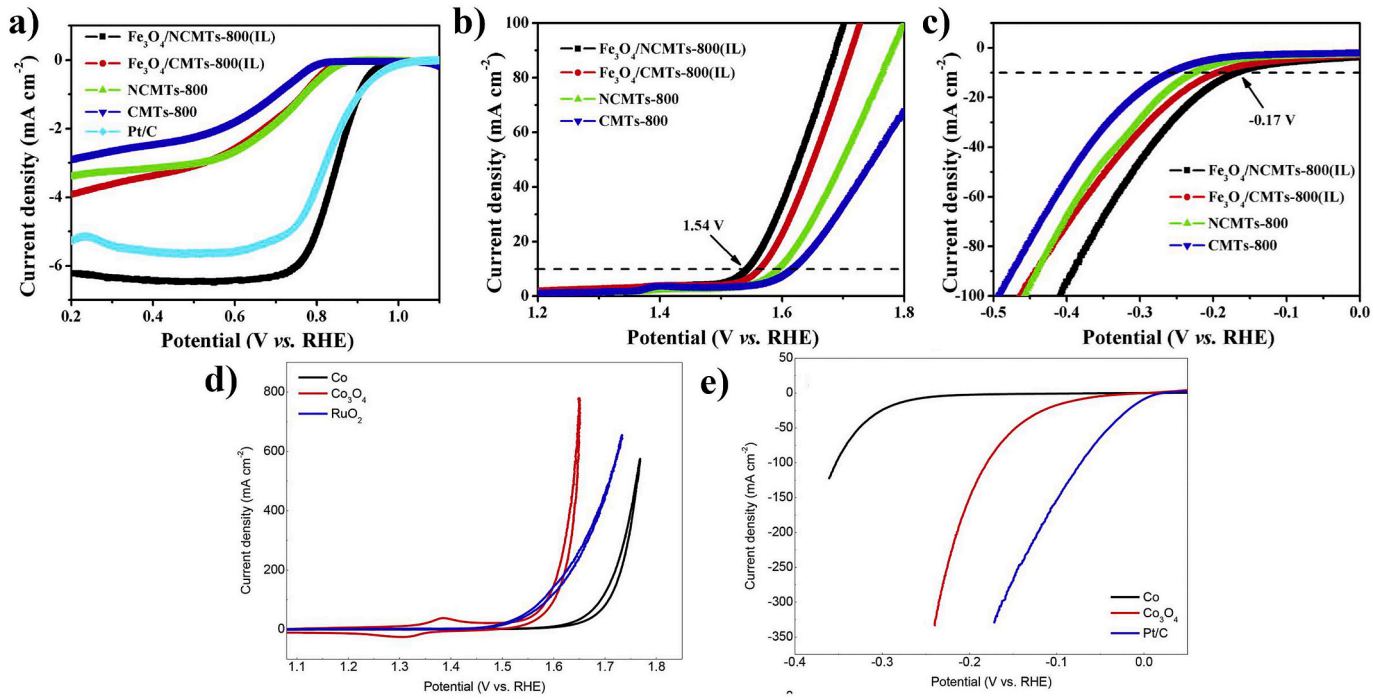

Fig. 9. Electroactivity of Fe_3O_4–based materials obtained from an iron ions-containing ionic liquid and supported on carbon materials (N-doped and undoped) in **a)** ORR, **b)** OER, and **c)** HER, respectively. Reprinted from Ref. 142. Copyright 2019, with permission from Elsevier. Electrochemical activity of Co_3O_4 octahedral particles, cobalt foam and Pt/C in **d)** OER and **e)** HER, respectively. Reprinted from Ref. 158. Copyright 2018, with permission from Elsevier.

synthesizing materials with oxygen vacancies and, thus, favoring the adsorption and dissociation of O_2. Moreover, they observed that vacancies were able to generate higher amounts of Co^{2+}, which is essential to form CoOOH species, the active site for OER.

Co_3O_4-based materials were also evaluated as bifunctional catalysts for OER and HER (Du et al., 2015, 2020; Wu et al., 2018a; Li et al., 2017). These oxides are often used alone (Du et al., 2020; Wu et al., 2018a) or with a small concentration of carbon material (Li et al., 2017) due to the poor activity that offers the latter component in both reactions. Du et al. (2020) studied the effect of oxygen vacancies in mesoporous Co_3O_4 nanoflowers and concluded that such structure provides high catalytic surface area and channels for ion diffusion. As expected, oxygen vacancies improve the electrical conductivity and favor the electron transfer. These vacancies could offer additional effects, such as promoting water adsorption and modulating the electronic structure, while the presence of surface hydroxide groups would favor HER and OER through water splitting (Fig. 9d and e) (Wu et al., 2018a). Du et al. (2015) synthesized also a nanocrystalline Co_3O_4 ink printed on carbon fiber paper. They associated the good activity to the higher number of active sites provided by nanoparticles and to the stronger interaction between the metal oxide nanoparticles and the carbon material, which favors the electron transfer improving OER and HER.

4.1. Spinel metal oxide-based materials with $A_xB_{3-x}O_4$ composition

This section focuses on the catalytic behavior of spinel metal oxide-based materials with a partial substitution of the transition metal according to the formula $A_xB_{3-x}O_4$ (A and B are *3d* transition metals). This strategy can be used to modify the physicochemical properties of the starting metal oxides and, as a result, opens the possibility of modulating the catalytic activity towards the electrochemical reactions of interest.

4.1.1. Spinel cobalt-based metal oxide materials with $M_xCo_{3-x}O_4$ composition

The partial substitution of cobalt by a divalent metal cation M^{2+} results in the modified spinel $M_xCo_{3-x}O_4$ (where M is usually Mn, Fe, Ni or Cu); this substitution generally improves the catalytic activity and stability of the Co_3O_4 compound. It was found that the crystal phase of the spinel metal oxide affects the catalytic activity and, in this context, the cubic phase is preferred because it provides a higher number of catalytic sites that may efficiently interact with O_2 (Lee et al., 2015a; Li et al., 2015a). Yang et al. (2019) studied different MCo_2O_4 spinels and found that $MnCo_2O_4$ exhibits better electrocatalytic behavior in ORR due to an alteration in the electronic structure of the cations (Fig. 10a). Moreover, Wei et al. (2017) observed that this metal oxide spinel offers an optimum filling of e_g orbitals, which favors ORR compared to other metal oxide spinels with a different Mn:Co ratio (Fig. 10b). $MnCo_2O_4$ shows activity in OER as well (Lankauf et al., 2020) and diverse studies focused on their bifunctionality (Shenghai et al., 2019; Cao et al., 2014, 2015). Metal oxides are usually supported on conductive materials to improve their activity. For example, Shenghai et al. (2019) synthesized $MnCo_2O_4$@C by combining a hydrothermal method with thermal decomposition. Such a synthesis procedure generates a particular morphology with higher specific surface area. The observed synergy between both components facilitates ORR and OER (Fig. 10c).

Regarding the substitution of Ni by Co, which generates a $NiCo_2O_4$ spinel, an enhancement of the catalytic activity towards ORR, OER, and HER was observed (Liu et al., 2019c; Gao et al., 2016; Béjar et al., 2019; Deng et al., 2017; Lim et al., 2019; Wei et al., 2019; Wang et al., 2016b) and, as a result, several works focused on its bifunctionality for ORR/OER (Béjar et al., 2019; Wang et al., 2016b) and OER/HER (Liu et al., 2019c; Gao et al., 2016; Deng et al., 2017). Increased catalytic activity was achieved through the synthesis of materials with specific porous structures or special morphology, which provide higher catalytic active sites. Particularly, Liu et al. (2019c) synthesized $NiCo_2O_{4-\delta}$ using a pulsed laser and obtained a material with enhanced electrocatalytic activity towards OER and OER. This effect was attributed to the modified morphology that generates both higher active surface area and Ni^{3+}/Ni^{2+} surface ratio. Another strategy to increase the activity consists on increasing the concentration of oxygen vacancies and several studies focused on this issue (Lim et al., 2019; Wei et al., 2019).

Finally, the substitution of Co by Cu yields $CuCo_2O_4$, a material that

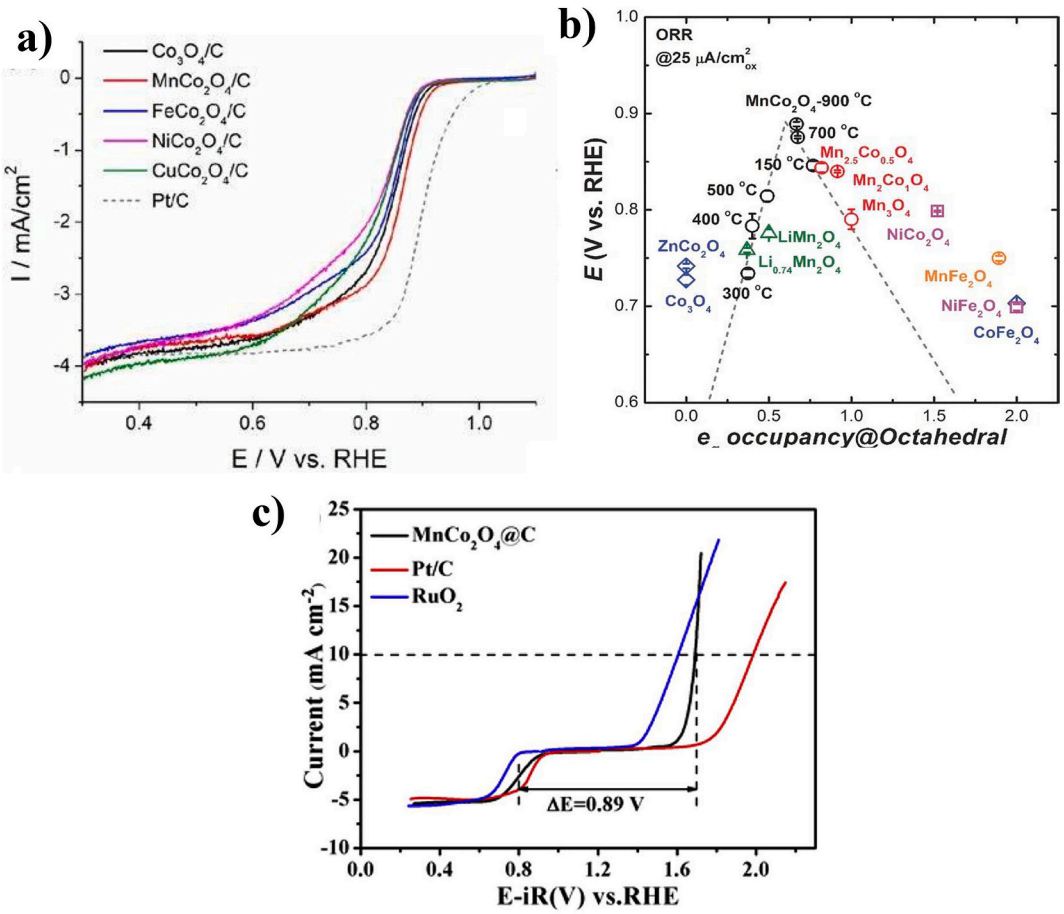

Fig. 10. a) Catalytic activity of metal oxides ACo_2O_4 (where A is Mn, Fe, Ni or Cu) in ORR. Reprinted from Ref. 161. **b)** Volcano plot of various spinel-based materials which relates the e_g orbital occupancy with the activity in ORR. Reprinted with permission from Ref. 162. Copyright 2017, John Wiley and Sons; **c)** Catalytic activity of $MnCo_2O_4$@C in ORR and OER. Reprinted from Ref. 164. Copyright 2019, with permission from Elsevier.

shows promising electrocatalytic activity towards ORR or OER and even HER (De Koninck et al., 2006, 2007; Serov et al., 2015; Cheng et al., 2017; Jia et al., 2010; Wang et al., 2016c). Indeed, a great effort was done to synthesize bifunctional catalysts for either ORR/OER (De Koninck et al., 2006, 2007; Serov et al., 2015; Cheng et al., 2017; Wang et al., 2016c) or OER/HER (Jia et al., 2010). In the latter case, materials not supported on carbon materials, such as $Ti/Cu_{0.3}Co_{2.7}O_4$, can be also employed. After the substitution of Co by Cu in Co_3O_4 spinels, Koninck et al. (De Koninck et al., 2006, 2007) observed better electrocatalytic response that was attributed to several factors. First, the introduction of Cu^{2+} increases the Co^{3+} concentration, thus enhancing the activity towards ORR because both species are active for O_2 adsorption. Second, the presence of copper improves the electrical conductivity. These combined effects enhance the overall OER kinetics. In the same way, in some studies hydrothermal methods (Wang et al., 2016c) and nanocasting with a silica template (Serov et al., 2015) were employed to provide higher surface area and to increase the catalytic activity. Cheng et al. (2017) succeeded in improving the catalytic activity using N-doped carbon nanotubes, which form Co–N or Cu–N species as active sites for ORR.

4.1.2. *Spinel iron-based metal oxide materials with $M_xFe_{3-x}O_4$ composition*

The effect of partial substitution of Fe in $M_xFe_{3-x}O_4$, where M is a *3d* transition metal, generally produces a positive effect on the catalytic activity towards the three reactions of interest. The catalytic activity can be modulated by selecting the appropriate metal cation. Zhu et al. (2013) studied the ORR on $M_xFe_{3-x}O_4$ (M = Fe, Cu, Co, Mn) nanoparticles supported on a carbon material. $MnFe_2O_4$ showed good activity towards ORR, which was associated to the activation of a Mn^{2+}/Mn^{3+} redox process at potentials close to the onset of oxygen reduction. However, $MnFe_2O_4$ showed poor activity under OER conditions and it was discarded as a bifunctional catalyst in favor of $CoFe_2O_4$ (Fig. 11a and b) (Si et al., 2017). There is no general agreement on the best $M_xFe_{3-x}O_4$ catalyst for OER among the Cu, Co and Ni series. In fact, Silva et al. (2019) reported that $CuFe_2O_4$ is the most active material, Li et al. (2015b) concluded that the best option is $CoFe_2O_4$ and Yuan et al. (2019b) found that $NiFe_2O_4$ is the best bifunctional catalyst for OER/HER because of its better electrical conductivity and higher electrocatalytic active surface area (Fig. 11c and d). Other authors suggested that $CoFe_2O_4$ and $NiFe_2O_4$ are the best options for OER/HER bifunctional catalysis (Bian et al., 2014; Xu et al., 2015b; Liu et al., 2016b; Chanda et al., 2015). Further research is necessary to understand if the lack of agreement is due to the differences in particle size, structure and surface composition achieved with the different synthetic methods used.

To discern which physicochemical properties can affect the ORR performance, Flores-Lasluisa et al., 2020b, 2022 studied the effect of the temperature in the post-calcination treatment after a solvothermal method in the synthesis of $CuFe_2O_4$- and $MnFe_2O_4$-based materials. For the $CuFe_2O_4$-based materials (Flores-Lasluisa et al., 2020b), it was observed that the crystal structure affects significantly the performance, being the cubic phase the most active. Moreover, the coexistence with other crystal phases such as CuO enhances the ORR activity due to a synergistic effect between both oxides. In the case of the $MnFe_2O_4$-based materials (Flores-Lasluisa et al., 2022), it was also observed that the crystal structure plays an important role in ORR together with the concentration of Mn^{3+} and Mn^{4+} species. It was reported that an excess

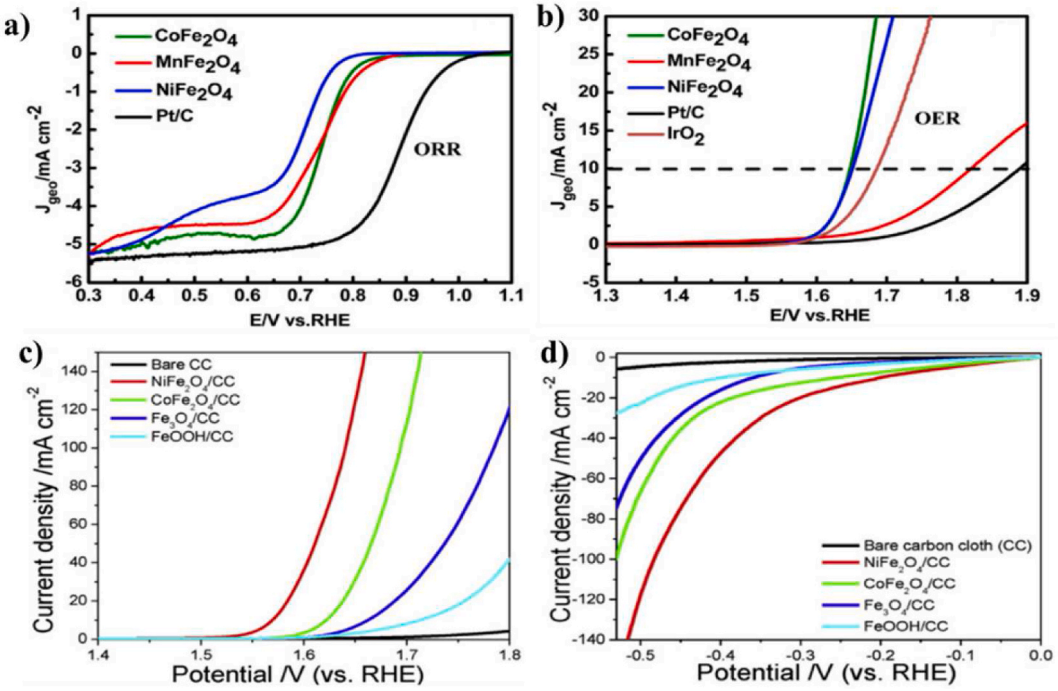

Fig. 11. Catalytic performance of $CoFe_2O_4$, $MnFe_2O_4$, and $CoFe_2O_4$ materials in **a)** ORR and **b)** OER. Reprinted from Ref. 181. Copyright 2017, with permission from Elsevier; Catalytic performance of $NiFe_2O_4$, $CoFe_2O_4$, and Fe-based materials in **c)** OER and **d)** HER. Reprinted from Ref. 184. Copyright 2019, with permission from Elsevier.

of Mn^{3+} can reduce the stability of the material because it can be oxidized to Mn^{4+} decreasing the number of active sites, thus an optimum concentration is required.

5. The effect of carbon material on the catalytic properties

Perovskite metal oxides and spinel metal oxides, likewise other metal oxides, have two main drawbacks when applied to electrochemical reactions (Hu et al., 2015; Vignesh et al., 2016; Zhu et al., 2013; Samanta and Raj, 2019). On the one hand, their particles are prone to agglomerate, which reduces the number of available active sites. On other hand, they exhibit poor electrical conductivity that makes the electron transfer difficult, thus reducing their catalytic activity. The number of active sites can be increased by synthesizing nanostructured materials (Kim et al., 2016; Park et al., 2015; Chai et al., 2017; Zhang et al., 2020e; Cheng et al., 2011) or with a porous structure (Li et al., 2018; Vignesh et al., 2016; Wang et al., 2019). However, in both cases it is necessary to support the metal oxides on other materials, to improve the electrical conductivity and, at the same time, increase the number of active sites exposed to the electrolytic medium. Carbon materials are excellent candidates to fulfil this role taking into account their interesting properties such as high electrical conductivity, high thermal stability, high surface area, and, in some cases, low price. Different types of carbon materials have been used for this purpose, such as carbon blacks (De Koninck et al., 2007; Kéranguéven et al., 2015), carbon nanotubes (Alexander et al., 2018; Zhang et al., 2020e; Li et al., 2019), graphene-based materials (Hu et al., 2015; Samanta and Raj, 2019; Rebekah et al., 2020; Zhuang et al., 2021), activated carbons (Hu et al., 2018; Flores-Lasluisa et al., 2019b) and nitrogen-doped carbon materials (Chen et al., 2017; Park et al., 2015; Najam et al., 2020; Wu et al., 2018b; Mathumba et al., 2020; Liu et al., 2021). Nevertheless, no sufficient attention is paid to the effect of the structure (at different levels) and surface chemistry of the carbon material on the interaction with the metal oxide and on its role on the catalytic activity improvement. This is a topic which requires further extensive research.

Both the nature and the morphology of the carbon materials are expected to have an important effect on the final catalytic performance of the perovskite- and spinel-based materials. Generally, carbon materials with large surface area and pore volumes are potential materials, as reported by Bo et al. (2015), which compared ordered mesoporous carbon materials with different structures, surface area, pore size and pore volume. It was observed that $NiCo_2O_4$ spinel nanoparticles synthesized in a carbon material with a high surface area and large pore volume produced the higher ORR activity because smaller nanoparticles were formed with a higher number of available active sites.

Ryabova et al. (2017) compared the electrocatalytic behavior of Mn_2O_3 spinel physically mixed with different carbon materials, such as carbon black (Vulcan, Ketjenblack 300 J and acetylene black), multi-wall carbon nanotubes, catalytic filamentous carbon and pyrolytic carbon materials. It was reported that carbon materials with a moderate specific surface area (Vulcan carbon black and pyrolytic carbons) maximize both the accessibility of the metal oxide surface for charge-transfer reactions and the extension of the oxide/carbon interface. It was also found that both edge and basal graphene planes should be exposed to the surface for better ORR performance. On the other hand, it seems that highly hydrophobic carbon materials (acetylene black and multi-wall carbon nanotubes) should be avoided to obtain more homogenous catalytic layers. Another interesting work conducted by Kéranguéven et al. (2020) reported important features of the carbon materials for higher catalytic performance. Metal oxides were synthesized by employing an in situ autocombustion method with the same carbon materials described above. In this case, it was reported that materials with a high degree of structural order can act as strong reducing agents. Thus, they can decrease the number of active sites by reducing the Mn species to non-catalytic species. In addition, the morphology of carbon materials affected to the growth of the metal oxides. For catalytic filamentous carbon, nanoparticles were formed between nanotube bundles, but also at the nanotube openings and probably inside carbon nanotubes, resulting in a small voltammetric charge due to a lower accessibility of the electrolyte to the metal oxide nanoparticles. For pyrolytic carbon materials, nanoparticles are formed in the shell-like pores thus becoming less accessible to oxygen, which

decreases the catalytic activity. Vulcan carbon black seems to be most suitable for this synthesis because its low porosity produces that the metal oxide nanoparticles are more accessible to oxygen. Kostuch et al. (2018) also reported that the carbon material influences positively the in situ synthesis of active manganese-cobalt spinel materials for ORR. Different carbon materials were used for this purpose, such as carbon blacks (Vulcan and Printex85), multi-wall carbon nanotubes (MWCNTs), mesoporous carbon and amorphous carbon. It was concluded that MWCNTs are the best support due to: i) higher dispersion of the nanocrystals on the surface and low particle agglomeration, ii) higher exposition of the (100) facets which provides higher number of active Co^{3+} and Mn^{3+} sites and iii) carbon materials with higher amorphous carbon content seems to favor peroxide formation.

Therefore, it can be concluded that there are some features of the carbon materials that can enhance the catalytic performance of the metal oxide: i) moderate specific surface area, ii) the presence of both edge and basal graphene planes, iii) hydrophobicity of the carbon materials, iv) low degree of structural order, v) good dispersion and accessibility of active nanoparticles, vi) low content of amorphous carbon, and vii) high electrical conductivity. However, not only the nature and morphology of the carbon materials can be determinant, but also other aspects that will be discussed below can strongly influence the catalytic performance. Several authors have suggested that a better electrocatalytic behavior of the metal oxide/carbon hybrid material compared to the individual materials is related to a synergistic effect resulting from the interaction of both materials (Li et al., 2016a; Lee et al., 2015b, 2015c; Park et al., 2015; Liang et al., 2011; Liu et al., 2014; Zhou et al., 2011; Chen et al., 2018). Lee at al (Lee et al., 2015b, 2015c). synthesized metal oxide perovskites in situ over diverse carbon materials. Among them, nanoparticles of $LaMn_{0.9}Co_{0.1}O_3$ obtained on carbon nanotubes were applied to ORR and OER (Fig. 12a and b, respectively). In both cases, a considerable improvement of catalytic activity was observed, which was attributed to a synergistic effect resulting from the interaction of both components. A similar synergistic effect was observed by Liang et al. (2011) after supporting Co_3O_4 nanocrystals on graphene. In this case, the enhancement of the catalytic activity towards ORR and OER was attributed to the formation of Co–N–C and Co–O–C species. Li et al. (2016a) suggested the formation of C–O–Mn species in $LaMnO_3$/C when in-situ synthesis was used, which would improve the electron transfer kinetics in the steps of ORR (see Fig. 12c that compares the in-situ synthesis with the physical mixing). The appearance of the strong interaction C–O-M was also observed when $LaMnO_3$ nanoparticles were mixed with carbon black for a subsequent heat treatment, which favors the intimate interaction between both components (Liu et al., 2014). Apart from the appearance of the synergistic effect, it is well known that non-doped carbon materials can catalyze ORR through a 2 + 2 electron mechanism (Zhu et al., 2017; Alexander et al., 2018; Mefford et al., 2019; Samanta and Raj, 2019; Poux et al., 2012). Particularly, these materials promote the reduction of O_2 to HO_2^- through Eq. 2, and the latter species can be then reduced by either disproportionation reaction (Eq. 4) or through the electrochemical reduction on the adjacent metal oxide material by a 2-electron pathway to give OH^- (Eq. 3) (Falcón et al., 2001).

Then, carbon materials may act as co-catalysts, thus favoring the formation of HO_2^- intermediates and, thus, improving the overall catalytic activity. However, they are less suitable for OER because their degradation occurs at the potential required for this reaction. Fortunately for some graphitic structures the kinetics is slow enough to show some long-term stability (Alexander et al., 2018). Apart from their role in improving electrical conductivity and providing larger number of active sites, carbon materials promote the release of active sites at the metal oxide by a spillover mechanism (Zhu et al., 2017). Specifically, O_2 generated over the active sites of the metal oxide may spill over the carbon material, thus releasing more active sites for further O_2 formation. Porous carbon materials, apart from their usual role of catalyst support, show high capacity to store hydrogen from the electrochemical reduction of water, which provides them with a fundamental advantage in HER catalysis (Blenda-Martínez et al., 2008; Leyva-García et al., 2014). Water molecules are adsorbed on the carbon material surface and subsequently they split into adsorbed H atoms (H_{ads}) and OH^- ions, then

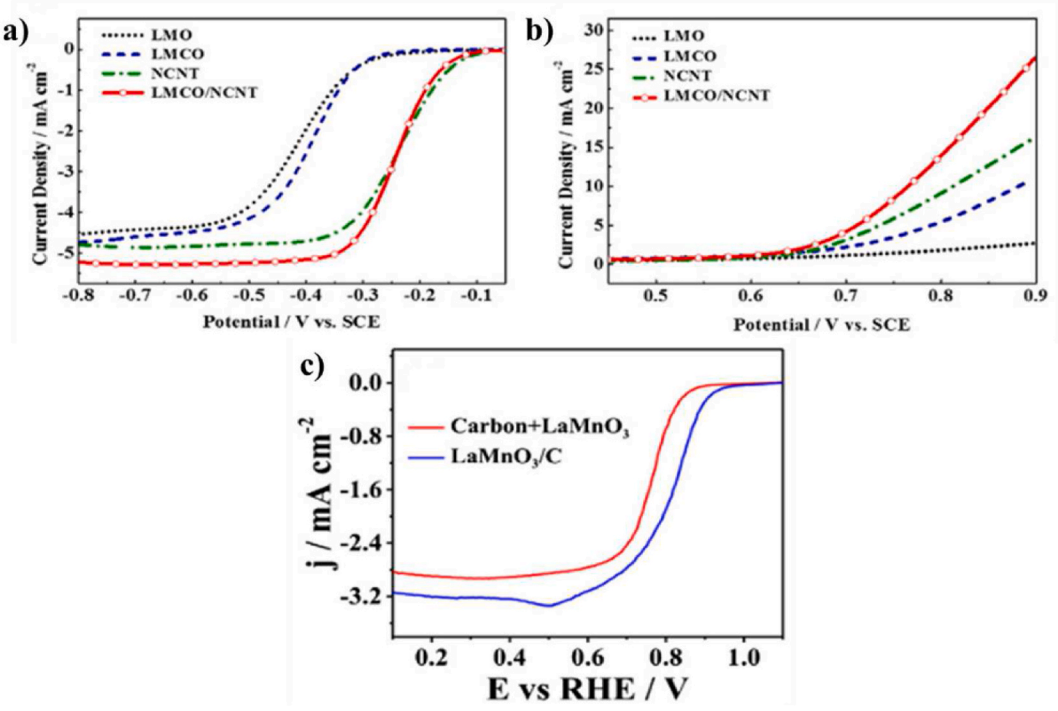

Fig. 12. Electrocatalytic performance of $LaMn_{0.9}Co_{0.1}O_3$ nanoparticles supported on N-doped carbon nanotubes in **a)** ORR and **b)** OER. Reprinted from Ref. 109. Copyright 2015, with permission from Elsevier; **c)** Effect of the in-situ synthesis of the $LaMnO_3$/C material. Reprinted from Ref. 68. Copyright 2016, with permission from Elsevier.

H_{ads} species can interact with reactive carbon atoms through the formation of reversible C–H bonds (Blenda-Martínez et al., 2008). Therefore, microporous porous carbons can act as a hydrogen reservoir providing H_{ads} species to the active sites of the metal oxide that catalyze the combination of the hydrogen species to form molecular hydrogen, thus enhancing the overall reaction.

6. Stability of metal oxide-based materials

The chemical and mechanical stability of heterogeneous catalysts is a pervasive issue in electrochemical processes. In addition to the search for higher efficiency, a great effort is being made in the development of perovskite and spinel-based metal oxides with high stability under alkaline conditions. Several studies (He et al., 2021; Deng et al., 2020; Tomon et al., 2021; Du et al., 2020) reported that the decrease in stability is related to changes in physicochemical properties such as morphology, crystal structure, particle agglomeration and, hence, changes in surface chemistry that strongly negatively affect the electrochemical performance. All these studies have been done in alkaline conditions because these materials are not chemically stable in acidic conditions.

The strategies followed to increase the stability of metal oxides are similar to those employed to improve their catalytic activity. It was reported that doping in A and B sites increases electrochemical performance because the presence of new elements promotes a morphological stabilization that, in addition, provides new active sites and redox pairs (Pawar et al., 2019; Shui et al., 2022; Qian et al., 2021; Shi et al., 2020). Qian et al. (2021) observed that Ca substitution in $LaCoO_3$ perovskite enhances the stability in ORR and OER by providing a more stable morphology and superior crystallinity without any agglomeration. In a previous communication Shi et al. (2020) suggested that the observed durability of ultrasmall spinel $Mn_xCo_{3-x}O_4$ nanoparticles is caused by the higher valence state of Mn and by the formation of a new metal-ion redox couple.

It has also been observed that modulation of the surface species of metal oxide materials can result in an improvement of their stability. Flores-Lasluisa et al. (2022) reported that $MnFe_2O_4$ solid nanospheres calcined at low temperature exhibit better ORR stability because of an optimum concentration of Mn^{3+} on the surface. As Mn^{3+} cations tend to oxidize to Mn^{4+} at the potential used for the stability test, a high concentration of this species could lead to the loss of activity. On the other hand, Matseke et al. (2020) observed that ultrasonication enhances the stability of $CoFe_2O_4$ in ORR because it favors the migration of cations to T-sites, which are more stable than O-sites in this spinel. Du et al. (2021) reported that A-site cationic defects in $LaMnO_3$ perovskite enhance the covalency of Mn–O bonds, thus optimizing the e_g orbital filling. Therefore, the high stability under ORR conditions was ascribed to the modulation of the electronic structure, which also provides more active sites available for this reaction.

The morphology of metal oxide materials seems also to influence their stability. The increased stability seems to be based on facilitating the release of gaseous products (O_2 and H_2) (Liu et al., 2019c; Lv et al., 2020). Lv et al. (2020) reported that the urchin-like nanostructure of the Al and P co-doped "superaerophobic" Co_3O_4 microspheres shows good stability for HER and OER because this structure favors the electrode-electrolyte contact and the transport of water drops to each part of the materials. Moreover, this material enhances the fast extraction of bubbles (H_2 and O_2), allowing the active sites to continue the electrochemical reactions.

Obviously, the agglomeration of metal oxide nanoparticles is detrimental to stability and decreases the number of active sites available. In many cases, the use of carbon materials in combination with the metal oxides resulted in an enhanced stability of catalysts. Several studies (He et al., 2021; Shenghai et al., 2019; Zhang et al., 2020e; Li et al., 2019; Zhuang et al., 2021; Xu et al., 2015c) reported that the intimate interaction between carbon materials and metal oxide favors charge transfer and slows down the catalyst degradation by avoiding the agglomeration of nanoparticles or the dissociation of the active phase. He et al. (2021) observed that the interconnected 3D Fe_3O_4/rGO composite, which consists of Fe_3O_4 nanoparticles anchored on graphene nanosheets, shows high stability in ORR. This behavior was explained in terms of its unique structure, which provides several advantages: i) large number of active sites, ii) suppression of the re-stacking of graphene and iii) lack of dissociation and aggregation of Fe_3O_4 nanoparticles due to the strong interaction between two components. Zhang et al. (2020e) reported a similar effect for Mn_3O_4 nanosheets coated on carbon nanotubes for ORR. The remarkable stability of this composite was related to the strong interaction between Mn_3O_4 and CNTs, which seemed to inhibit dissociation and migration of the metal oxide through the interfacial products. Several authors proposed a solution to avoid the agglomeration of nanoparticles by coating the nanoparticles with carbon materials. This strategy prevents aggregation but, in addition, facilitates the electron transfer (Shenghai et al., 2019; Wang et al., 2022). In particular, Wang et al. (2022) synthesized $CoFe_2O_4$ nanoparticles embedded in N-doped carbon nanotubes and found low particle aggregation and detachment, resulting in good ORR stability. The protection mechanism seems to be associated with the wrapping of nanoparticles by the CNT layer.

7. Overview and perspectives

Electrochemical devices for energy conversion such as fuel cells, metal-air batteries or electrolyzers are considered as promising alternatives to fossil fuel technologies for a more sustainable and eco-friendly development of society. The main challenge before their final implementation is the substitution of current catalytic materials, which are based on scarce noble metals. Therefore, an effort is required to develop catalysts based on more abundant and less expensive elements that may reach similar performance. Among these materials, metal oxides with perovskite and spinel-based structures stand out due to their properties and they deserve scientific attention.

Perovskite metal oxides with $LaBO_3$ structure appeared as alternatives for ORR and OER. $LaMnO_3$ and $LaCoO_3$ show good activity under ORR conditions, whereas $LaCoO_3$ and $LaNiO_3$ are more appropriate for OER. To improve their electrocatalytic performance, a partial substitution of B cations can be done. This generates more active sites and creates oxygen vacancies that enhances electrical conductivity and electron transfer kinetics. In addition, partial substitution of lanthanum by divalent cations is possible, thus generating more oxygen vacancies and number of surface active sites. For these reasons, perovskite metal oxide materials based on the formula $La_{1-x}A'_xB_{1-y}B'_yO_3$, where A′ is an alkaline-earth metal and both B and B′ are *3d* transition metals, can be optimized for both ORR and OER.

Regarding materials with spinel-based structure, they can be classified according to their composition into two groups: those formed by a single transition metal and those formed by two of them (B_3O_4 and AB_2O_4, respectively). Among the first group, Co_3O_4 exhibits good behavior towards the three reactions of interest (ORR, OER, and HER). In the second group an optimization of the composition is required to obtain a suitable bifunctional behavior. In this way, when Mn is included as the A cation ($MnCo_2O_4$), an appropriate response is obtained for ORR, whereas its activity in OER and HER can be enhanced by introducing Ni or Cu. Similarly, $MnFe_2O_4$ spinel offers the best response for ORR, whereas $CoFe_2O_4$ and $NiFe_2O_4$ materials seem more interesting options for OER and HER.

The electrocatalytic activity of metal oxides can be improved by mixing them with carbon materials. This is due to several factors, such as the increase in both electrical conductivity and number of accessible catalytic sites, and to the appearance of a synergistic effect between both components. Carbon materials can act as co-catalysts for ORR, by assisting the reduction of molecular oxygen to HO_2^-. This intermediate is then reduced to OH^- on active sites adjacent to the metal oxide. For

OER, carbon materials may help in the regeneration of the active sites on the oxide material through the spillover of O_2 and, finally, porous carbon materials can store hydrogen thus promoting the HER reaction.

Unfortunately, the main ORR mechanism in electrodes made from undoped carbon materials is the two-electron pathway, in which hydrogen peroxide is generated. This is an undesirable reaction due to the loss of energy efficiency of the fuel cell and its corrosive nature. To favor the four-electron mechanism, the most studied approach is the modification of the surface chemistry of the carbon materials by including functionalities able to modify properties and reactivity. As an example, carbon materials doped with nitrogen functional groups are one of the most promising alternatives for applications in fuel cells, since nitrogen is capable of generating active sites in neighboring carbon atoms, thus facilitating the adsorption of the oxygen molecule as a first stage prior to its reduction. Therefore, the combination of metal oxides with functionalized carbon materials and a thorough understanding of the synergistic effect between the two materials are topics that deserve a research effort. In addition, the use of metal oxides as electrocatalysts involves their synthesis in the form of nanoparticles, whose properties could be substantially benefited if they are combined with functionalized, high surface area nanostructured carbon materials. Although reported metal oxide-based nanoparticles show high electrocatalytic performance in electrochemical reactions, these materials are typically larger than 20 nm in size. The development of 5–10 nm sized nanoparticles is required to maximize activity, because higher number of surface active sites available for reactions are provided. Therefore, new synthesis methods are needed to obtain smaller nanoparticles that can significantly improve the electroactivity of these materials.

The development of carbon materials showing high activity through peroxide generation deserves attention because they can act also as co-catalysts for ORR. Since the B–N–C bond plays an important role in O_2 adsorption, an interesting subject for future studies could be the substitution of nitrogen centers by other heteroatoms such as phosphorus or boron, which were reported to promote good catalytic responses (Quílez-Bermejo et al., 2020). On the other hand, since the stability of metal oxides under working conditions is mandatory, a challenging goal could be the synthesis of materials showing improved stability in acidic media. Attaining this objective would increase the applicability of these alternative catalyts in fuel cells and electrolyzer devices. It is also worth noting that transition metal oxides show good performance when tested in laboratory by electrochemical techniques such as cyclic voltammetry or linear scanning voltammetry but, their implementation in practical devices is not yet well developed.

Credit author statement

Authors contributed equally to this work.

Declaration of competing interest

The authors declare that they have no known competing financial interests or personal relationships that could have appeared to influence the work reported in this paper.

Acknowledgements

The authors thank to the Ministerio de Ciencia e Innovación/AEI (PID 2019-105923RB-I00) for financial support. J.X.F.-L. gratefully acknowledges MINECO for financial support through an FPI contract (BES-2017-081598).

References

Abdol Rahim, A.H., Tijani, A.S., Kamarudin, S.K., Hanapi, S., 2016. An overview of polymer electrolyte membrane electrolyzer for hydrogen production: modeling and mass transport. J. Power Sources 309, 56–65. https://doi.org/10.1016/j.jpowsour.2016.01.012.

Abe, Y., Satoh, I., Saito, T., Kan, D., Shimakawa, Y., 2020. Oxygen reduction reaction catalytic activities of pure Ni-based perovskite-related structure oxides. Chem. Mater. 32, 8694–8699. https://doi.org/10.1021/acs.chemmater.0c03320.

Alegre, C., Modica, E., Aricò, A.S., Baglio, V., 2018. Bifunctional oxygen electrode based on a perovskite/carbon composite for electrochemical devices. J. Electroanal. Chem. 808, 412–419. https://doi.org/10.1016/j.jelechem.2017.06.023.

Alexander, C.T., Abakumov, A.M., Forslund, R.P., Johnston, K.P., Stevenson, K.J., 2018. Role of the carbon support on the oxygen reduction and evolution activities in $LaNiO_3$ composite electrodes in alkaline solution. ACS Appl. Energy Mater. 1, 1549–1558. https://doi.org/10.1021/acsaem.7b00339.

Andújar, J.M., Segura, F., 2009. Fuel cells: history and updating. A walk along two centuries. Renew. Sustain. Energy Rev. 13, 2309–2322. https://doi.org/10.1016/j.rser.2009.03.015.

Aoki, Y., Tsuji, E., Motohashi, T., Kowalski, D., Habazaki, H., 2018. $La_{0.7}Sr_{0.3}Mn1–xNixO3–\delta$ electrocatalysts for the four-electron oxygen reduction reaction in concentrated alkaline media. J. Phys. Chem. C 122, 22301–22308. https://doi.org/10.1021/acs.jpcc.8b06741.

Ashok, A., Kumar, A., Bhosale, R.R., Almomani, F., Malik, S.S., Suslov, S., Tarlochan, F., 2018. Combustion synthesis of bifunctional $LaMO_3$ (M = Cr, Mn, Fe, Co, Ni) perovskites for oxygen reduction and oxygen evolution reaction in alkaline media. J. Electroanal. Chem. 809, 22–30. https://doi.org/10.1016/j.jelechem.2017.12.043.

Béjar, J., Álvarez-Contreras, L., Ledesma-García, J., Arjona, N., Arriaga, L.G., 2019. Electrocatalytic evaluation of Co_3O_4 and $NiCo_2O_4$ rosettes-like hierarchical spinel as bifunctional materials for oxygen evolution (OER) and reduction (ORR) reactions in alkaline media. J. Electroanal. Chem. 847, 113190 https://doi.org/10.1016/j.jelechem.2019.113190.

Bian, W., Yang, Z., Strasser, P., Yang, R., 2014. A $CoFe_2O_4$/graphene nanohybrid as an efficient bi-functional electrocatalyst for oxygen reduction and oxygen evolution. J. Power Sources 250, 196–203. https://doi.org/10.1016/j.jpowsour.2013.11.024.

Bleda-Martínez, M.J., Pérez, J.M., Linares-Solano, A., Morallón, E., Cazorla-Amorós, D., 2008. Effect of surface chemistry on electrochemical storage of hydrogen in porous carbon materials. Carbon 46, 1053–1059. https://doi.org/10.1016/j.carbon.2008.03.016.

Bo, X., Zhang, Y., Li, M., Nsabimana, A., Guo, L., 2015. $NiCo_2O_4$ spinel/ordered mesoporous carbons as noble-metal free electrocatalysts for oxygen reduction reaction and the influence of structure of catalyst support on the electrochemical activity of $NiCo_2O_4$. J. Power Sources 288, 1–8. https://doi.org/10.1016/j.jpowsour.2015.04.110.

Bockris, J.O., Otagawa, T., 1984. The electrocatalysis of oxygen evolution on perovskites. J. Electrochem. Soc. 131, 290. https://doi.org/10.1149/1.2115565.

Bradley, K., Giagloglou, K., Hayden, B.E., Jungius, H., Vian, C., 2019. Reversible perovskite electrocatalysts for oxygen reduction/oxygen evolution. Chem. Sci. 10, 4609–4617. https://doi.org/10.1039/c9sc00412b.

Cao, X., Jin, C., Lu, F., Yang, Z., Shen, M., Yang, R., 2014. Electrochemical properties of $MnCo_2O_4$ spinel bifunctional catalyst for oxygen reduction and evolution reaction. J. Electrochem. Soc. 161, H296–H300. https://doi.org/10.1149/2.029405jes.

Cao, X., Yan, W., Jin, C., Tian, J., Ke, K., Yang, R., 2015. Surface modification of $MnCo_2O_4$ with conducting polypyrrole as a highly active bifunctional electrocatalyst for oxygen reduction and oxygen evolution reaction. Electrochim. Acta 180, 788–794. https://doi.org/10.1016/j.electacta.2015.08.160.

Celorrio, V., Dann, E., Calvillo, L., Morgan, D.J., Hall, S.R., Fermin, D.J., 2016a. Oxygen reduction at carbon-supported lanthanides: the role of the B-site. Chemelectrochem 3, 283–291. https://doi.org/10.1002/celc.201500440.

Celorrio, V., Calvillo, L., Dann, E., Granozzi, G., 2016b. Oxygen reduction reaction at $La_xCa_{1-x}MnO_3$ nanostructures: interplay between A-site segregation and B-site valency. Catal. Sci. Technol. 6, 7231–7238. https://doi.org/10.1039/c6cy01105e.

Celorrio, V., Calvillo, L., Granozzi, G., Russell, A.E., Fermin, D.J., 2018. $AMnO_3$ (A = Sr, La, Ca, Y) perovskite oxides as oxygen reduction electrocatalysts. Top. Catal. 61, 154–161. https://doi.org/10.1007/s11244-018-0886-5.

Chai, H., Xu, J., Han, Ji, Su, Y., Sun, Z., Jia, D., Zhou, W., 2017. Facile synthesis of Mn_3O_4-rGO hybrid materials for the high-performance electrocatalytic reduction of oxygen. J. Colloid Interface Sci. 488, 251–257. https://doi.org/10.1016/j.jcis.2016.10.049.

Chanda, D., Hnát, J., Paidar, M., Schauer, J., Bouzek, K., 2015. Synthesis and characterization of $NiFe_2O_4$ electrocatalyst for the hydrogen evolution reaction in alkaline water electrolysis using different polymer binders. J. Power Sources 285, 217–226. https://doi.org/10.1016/j.jpowsour.2015.03.067.

Chawla, N., 2019. Recent advances in air-battery chemistries, Mater. Today Chem 12, 324–331. https://doi.org/10.1016/j.mtchem.2019.03.006.

Chel, A., Kaushik, G., 2018. Renewable energy technologies for sustainable development of energy efficient building. Alex. Eng. J. 57, 655–669. https://doi.org/10.1016/j.aej.2017.02.027.

Chen, D., Chen, C., Baiyee, Z.M., Shao, Z., Ciucci, F., 2015. Nonstoichiometric oxides as low-cost and highly-efficient oxygen reduction/evolution catalysts for low-temperature electrochemical devices. Chem. Rev. 115, 9869–9921. https://doi.org/10.1021/acs.chemrev.5b00073.

Chen, X., Chen, S., Nan, B., Jia, F., Lu, Z., Deng, H., 2017. In situ, facile synthesis of $La_{0.8}Sr_{0.2}MnO_3$/nitrogen-doped graphene: a high-performance catalyst for rechargeable Li-O_2 batteries. Ionics 23, 2241–2250. https://doi.org/10.1007/s11581-017-2079-9.

Chen, M., Wang, L., Yang, H., Zhao, S., Xu, H., Wu, G., 2018. Nanocarbon/oxide composite catalysts for bifunctional oxygen reduction and evolution in reversible alkaline fuel cells: a mini review. J. Power Sources 375, 277–290. https://doi.org/10.1016/j.jpowsour.2017.08.062.

Cheng, F., Shen, J., Peng, B., Pan, Y., Tao, Z., Chen, J., 2011. Rapid room-temperature synthesis of nanocrystalline spinels as oxygen reduction and evolution electrocatalysts. Nat. Chem. 3, 79–84. https://doi.org/10.1038/nchem.931.

Cheng, H., Li, M.L., Su, C.Y., Li, N., Liu, Z.Q., 2017. Cu-Co bimetallic oxide quantum dot decorated nitrogen-doped carbon nanotubes: a high-efficiency bifunctional oxygen electrode for Zn–air batteries. Adv. Funct. Mater. 27, 1–10. https://doi.org/10.1002/adfm.201701833.

David, M., Ocampo-Martínez, C., Sánchez-Peña, R., 2019. Advances in alkaline water electrolyzers: a review. J. Energy Storage 23, 392–403. https://doi.org/10.1016/j.est.2019.03.001.

De Koninck, M., Poirier, S.-C., Marsan, B., 2006. $Cu_xCo_{3-x}O_4$ used as bifunctional electrocatalyst. J. Electrochem. Soc. 153, A2103. https://doi.org/10.1149/1.2338631.

De Koninck, M., Poirier, S.-C., Marsan, B., 2007. $Cu_xCo_{3-x}O_4$ used as bifunctional electrocatalyst. J. Electrochem. Soc. 154, A381. https://doi.org/10.1149/1.2454366.

de Villiers, J.P.R., Buseck, P.R., 2003. Mineralogy and instrumentation. In: Meyers, R.A. (Ed.), Encyclopedia of Physical Science and Technology, third ed. Academic Press, New York, pp. 1–27. https://doi.org/10.1016/B0-12-227410-5/00451-8.

Dekel, D.R., 2018. Review of cell performance in anion exchange membrane fuel cells. J. Power Sources 375, 158–169. https://doi.org/10.1016/j.jpowsour.2017.07.117.

Deng, J., Zhang, H., Zhang, Y., Luo, P., Liu, L., Wang, Y., 2017. Striking hierarchical urchin-like peapoded $NiCo_2O_4$@C as advanced bifunctional electrocatalyst for overall water splitting. J. Power Sources 372, 46–53. https://doi.org/10.1016/j.jpowsour.2017.10.062.

Deng, Y., Tian, X., Shen, G., Gao, Y., Lin, C., Ling, L., 2020. Coupling hollow Fe_3O_4 nanoparticles with oxygen vacancy on mesoporous carbon as a high-efficiency ORR electrocatalyst for Zn-air battery. J. Colloid Interface Sci. 567, 410–418. https://doi.org/10.1016/j.jcis.2020.02.013.

Du, S., Ren, Z., Zhang, J., Wu, J., Xi, W., Zhu, J., Fu, H., 2015. Co_3O_4 nanocrystals ink printing on carbon fiber paper as large-area electrode for electrochemical water splitting. Chem 51, 8066–8069. https://doi.org/10.1039/C5CC01080B.

Du, J., Li, C., Tang, Q., 2020. Oxygen vacancies enriched Co_3O_4 nanoflowers with single layer porous structures for water splitting. Electrochim. Acta 331, 135456. https://doi.org/10.1016/j.electacta.2019.135456.

Du, D., Zheng, R., He, M., Zhao, C., Zhou, B., Li, R., Xu, H., Wen, X., Zeng, T., Shu, C., 2021. A-site cationic defects induced electronic structure regulation of $LaMnO_3$ perovskite boosts oxygen electrode reactions in aprotic lithium–oxygen batteries. Energy Storage Mater. 43, 293–304. https://doi.org/10.1016/j.ensm.2021.09.011.

Eftekhari, A., 2017. Tuning the electrocatalysts for oxygen evolution reaction. Mater. Today Energy 5, 37–57. https://doi.org/10.1016/j.mtener.2017.05.002.

Falcón, H., Carbonio, R., Fierro, J.L., 2001. Correlation of oxidation states in $LaFe_xNi_{1-x}O_{3+\delta}$ oxides with catalytic activity for H_2O_2 decomposition. J. Catal. 203, 264–272. https://doi.org/10.1006/jcat.2001.3351.

Flores-Lasluisa, J.X., Huerta, F., Cazorla-Amorós, D., Morallón, E., 2019a. Structural and morphological alterations induced by cobalt substitution in $LaMnO_3$ perovskites. J. Colloid Interface Sci. 556, 658–666. https://doi.org/10.1016/j.jcis.2019.08.112.

Flores-Lasluisa, J.X., Quílez-Bermejo, J., Ramírez-Pérez, A.C., Huerta, F., Cazorla-Amorós, D., Morallón, E., 2019b. Copper-doped cobalt spinel electrocatalysts supported on activated carbon for hydrogen evolution reaction. Materials 12, 1302. https://doi.org/10.3390/ma12081302.

Flores-Lasluisa, J.X., Huerta, F., Cazorla-Amorós, D., Morallon, E., 2020a. Carbon material and cobalt-substitution effects in the electrochemical behavior of $LaMnO_3$ for ORR and OER. Nanomaterials 10, 2394. https://doi.org/10.3390/nano10122394.

Flores-Lasluisa, J.X., Salinas-Torres, D., López-Ramón, M.V., Álvarez, M.A., Moreno-Castilla, C., Cazorla-Amorós, D., Morallón, E., 2020b. Copper ferrite nanospheres composites mixed with carbon black to boost the oxygen reduction reaction. Colloids Surfaces A Physicochem. Eng. Asp. 613, 126060 https://doi.org/10.1016/j.colsurfa.2020.126060.

Flores-Lasluisa, J.X., Salinas-Torres, D., López-Ramón, M.V., Moreno-Castilla, C., Álvarez, M.A., Morallón, E., Cazorla-Amorós, D., 2022. Electrocatalytic activity of calcined manganese ferrite solid nanospheres in the oxygen reduction reaction. Environ. Res. 204, 112126 https://doi.org/10.1016/j.envres.2021.112126.

Gao, S., Geng, K., 2014. Facile construction of Mn_3O_4 nanorods coated by a layer of nitrogen-doped carbon with high activity for oxygen reduction reaction. Nano Energy 6, 44–50. https://doi.org/10.1016/j.nanoen.2014.02.013.

Gao, X., Zhang, H., Li, Q., Yu, X., Hong, Z., Zhang, X., Liang, C., Lin, Z., 2016. Hierarchical $NiCo_2O_4$ hollow microcuboids as bifunctional electrocatalysts for overall water-splitting. Angew. Chemie - Int. Ed. 55, 6290–6294. https://doi.org/10.1002/anie.201600525.

Goswami, C., Hazarika, K.K., Bharali, P., 2018. Transition metal oxide nanocatalysts for oxygen reduction reaction. Mater. Sci. Energy Technol. 1, 117–128. https://doi.org/10.1016/j.mset.2018.06.005.

Griffith, J.S., Orgel, L.E., 1957. Ligand-field theory. Q. Rev. Chem. Soc. 11, 381. https://doi.org/10.1039/qr9571100381.

Grimaud, A., May, K.J., Carlton, C.E., Lee, Y.L., Risch, M., Hong, W.T., Zhou, J., Shao-Horn, Y., 2013. Double perovskites as a family of highly active catalysts for oxygen evolution in alkaline solution. Nat. Commun. 4, 1–7. https://doi.org/10.1038/ncomms3439.

Grimes, R.W., Anderson, A.B., Heuer, A.H., 1989. Predictions of cation distributions in AB_2O_4 spinels from normalized ion energies. J. Am. Chem. Soc. 111, 1–7. https://doi.org/10.1021/ja00183a001.

Guo, J., Li, Q., Hou, H., Chen, J., Wang, C., Zhang, S., Wang, X., 2019. Cost-effective Co_3O_4 nanospheres on nitrogen- doped graphene used as highly efficient catalyst for oxygen reduction reaction. Int. J. Hydrogen Energy 44, 30348–30356. https://doi.org/10.1016/j.ijhydene.2019.09.165.

He, X., Long, X., Wang, P., Wu, H., Han, P., Tang, Y., Li, K., Ma, X., Zhang, Y., 2021. Interconnected 3D Fe_3O_4/rGO as highly durable electrocatalyst for oxygen reduction reaction. J. Alloys Compd. 855, 157422 https://doi.org/10.1016/j.jallcom.2020.157422.

Hong, W.T., Risch, M., Stoerzinger, K.A., Grimaud, A., Suntivich, J., Shao-Horn, Y., 2015. Toward the rational design of non-precious transition metal oxides for oxygen electrocatalysis. Energy Environ. Sci. 8, 1404–1427. https://doi.org/10.1039/C4EE03869J.

Hu, J., Wang, L., Shi, L., Huang, H., 2015. Oxygen reduction reaction activity of $LaMn_{1-x}Co_xO_3$-graphene nanocomposite for zinc-air battery. Electrochim. Acta 161, 115–123. https://doi.org/10.1016/j.electacta.2015.02.048.

Hu, J., Shi, Z., Su, C., Lu, B., Shao, Z., Huang, H., 2018. Anchoring perovskite $LaMnO_3$ nanoparticles on biomass−derived N, P co−doped porous carbon for efficient oxygen reduction. Electrochim. Acta 274, 40–48. https://doi.org/10.1016/j.electacta.2018.04.081.

Hu, S., Ni, W., Yang, D., Ma, C., Zhang, J., Duan, J., 2020. Fe_3O_4 nanoparticles encapsulated in single-atom Fe-N-C towards ef fi cient oxygen reduction reaction : effect of the micro and macro pores. Carbon 162, 245–255. https://doi.org/10.1016/j.carbon.2020.02.059.

Hua, B., Li, M., Zhang, Y.-Q., Sun, Y.-F., Luo, J.-L., 2017. All-in-one perovskite catalyst: smart controls of architecture and composition toward enhanced oxygen/hydrogen evolution reactions. Adv. Energy Mater. 7, 1700666 https://doi.org/10.1002/aenm.201700666.

Huang, J., Wang, Y., 2020. Efficient renewable-to-hydrogen conversion via decoupled electrochemical water splitting. Cell Reports Phys. Sci. 1, 100138 https://doi.org/10.1016/j.xcrp.2020.100138.

Hurley, P., 2002. Build Your Own Fuel cells. Wheelock Mountain Publications, Wheelok VT, USA.

Hyodo, T., Hayashi, M., Miura, N., Yamazoe, N., 1996. Catalytic activities of rare-earth manganites for cathodic reduction of oxygen in alkaline solution. J. Electrochem. Soc. 143, L266–L267. https://doi.org/10.1149/1.1837229.

Janani, G., Chae, Y., Surendran, S., Sim, Y., Park, W., Kim, J.K., Sim, U., 2020. Rational design of spinel oxide nanocomposites with tailored electrochemical oxygen evolution and reduction reactions for zinc-air batteries. Appl. Sci. 10, 1–21. https://doi.org/10.3390/app10093165.

Ji, Q., Bi, L., Zhang, J., Cao, H., Zhao, X.S., 2020. The role of oxygen vacancies of ABO_3 perovskite oxides in the oxygen reduction reaction. Energy Environ. Sci. 13, 1408–1428. https://doi.org/10.1039/d0ee00092b.

Jia, J., Li, X., Chen, G., 2010. Stable spinel type cobalt and copper oxide electrodes for O_2 and H_2 evolutions in alkaline solution. Electrochim. Acta 55, 8197–8206. https://doi.org/10.1016/j.electacta.2010.04.026.

Jia, X., Gao, S., Liu, T., Li, D., Tang, P., Feng, Y., 2017. Controllable synthesis and Bi-functional electrocatalytic performance towards oxygen electrode reactions of Co_3O_4/N-rgo composites. Electrochim. Acta 226, 104–112. https://doi.org/10.1016/j.electacta.2016.12.191.

Jia, X., Zhang, Y., Zhang, L., Wang, L., Zhou, L., 2019. Controllable synthesis and bi-functional electrocatalytic performance towards oxygen electrocatalytic reactions of Co_3O_4 nanoflakes/nitrogen-doped modified CMK-3 nanocomposite. Inorg. Chem. Commun. 108, 107524 https://doi.org/10.1016/j.inoche.2019.107524.

Kéranguéven, G., Royer, S., Savinova, E., 2015. Synthesis of efficient Vulcan-$LaMnO_3$ perovskite nanocomposite for the oxygen reduction reaction. Electrochem. Commun. 50, 28–31. https://doi.org/10.1016/j.elecom.2014.10.019.

Kéranguéven, G., Ulhaq-Bouillet, C., Papaefthimiou, V., Royer, S., Savinova, E., 2017. Perovskite-carbon composites synthesized through in situ autocombustion for the oxygen reduction reaction: the carbon effect. Electrochim. Acta 245, 156–164. https://doi.org/10.1016/j.electacta.2017.05.113.

Kéranguéven, G., Bouillet, C., Papaefthymiou, V., Simonov, P.A., Savinova, E.R., 2020. How key characteristics of carbon materials influence the ORR activity of $LaMnO_3$- and Mn_3O_4-carbon composites prepared by in situ autocombustion method. Electrochim. Acta 353. https://doi.org/10.1016/j.electacta.2020.136557.

Kalubarme, R.S., Park, G.-E., Jung, K.-N., Shin, K.-H., Ryu, W.-H., Park, C.-J., 2014. $LaNi_xCo_{1-x}O_{3-\delta}$ perovskites as catalyst material for non-aqueous lithium-oxygen batteries. J. Electrochem. Soc. 161, A880–A889. https://doi.org/10.1149/2.012406jes.

Kaufman, G.B., 1993. Inorganic chemistry: principles of structure and reactivity, 4th ed. (Huheey, james E.; keiter, ellen A.; keiter, richard L.). J. Chem. Educ. 70, A279. https://doi.org/10.1021/ed070pA279.1.

Kemppainen, E., Bodin, A., Sebok, B., Pedersen, T., Seger, B., Mei, B., Bae, D., Vesborg, P. C.K., Halme, J., Hansen, O., Lund, P.D., Chorkendorff, I., 2015. Scalability and feasibility of photoelectrochemical H_2 evolution: the ultimate limit of Pt nanoparticle as an HER catalyst. Energy Environ. Sci. 8, 2991–2999. https://doi.org/10.1039/c5ee02188j.

Kim, W.S., Anoop, G., Lee, H.J., Lee, S.S., Kwak, J.H., Lee, H.J., Jo, J.Y., 2016. Facile synthesis of perovskite $LaMnO_{3+\delta}$ nanoparticles for the oxygen reduction reaction. J. Catal. 344, 578–582. https://doi.org/10.1016/j.jcat.2016.10.029.

Kongkanand, A., Gu, W., Mathias, M.F., 2019. Proton-exchange membrane fuel cells with low-Pt content. In: Fuel Cells and Hydrogen Production, Encyclopedia of Sustainability Science and Technology Series. Springer, New York. https://doi.org/10.1007/978-1-4939-7789-5.

Kostuch, A., Gryboś, J., Indyka, P., Osmieri, L., Specchia, S., Sojka, Z., Kruczała, K., 2018. Morphology and dispersion of nanostructured manganese-cobalt spinel on various carbon supports: the effect on the oxygen reduction reaction in alkaline media. Catal. Sci. Technol. 8, 642–655. https://doi.org/10.1039/c7cy02228j.

Kozuka, H., Ohbayashi, K., Koumoto, K., 2015. Electronic conduction in La-based perovskite-type oxides. Sci. Technol. Adv. Mater. 16, 026001 https://doi.org/10.1088/1468-6996/16/2/026001.

Lankauf, K., Cysewska, K., Karczewski, J., Mielewczyk-Gryń, A., Górnicka, K., Cempura, G., Chen, M., Jasiński, P., Molin, S., 2020. $Mn_xCo_{3-x}O_4$ spinel oxides as efficient oxygen evolution reaction catalysts in alkaline media. Int. J. Hydrogen Energy 45, 14867–14879. https://doi.org/10.1016/j.ijhydene.2020.03.188.

Lee, E., Jang, J.H., Kwon, Y.U., 2015a. Composition effects of spinel $Mn_xCo_{3-x}O_4$ nanoparticles on their electrocatalytic properties in oxygen reduction reaction in alkaline media. J. Power Sources 273, 735–741. https://doi.org/10.1016/j.jpowsour.2014.09.156.

Lee, D.U., Park, H.W., Park, M.G., Ismayilov, V., Chen, Z., 2015b. Synergistic bifunctional catalyst design based on perovskite oxide nanoparticles and intertwined carbon nanotubes for rechargeable zinc–air battery applications. ACS Appl. Mater. Interfaces 7, 902–910. https://doi.org/10.1021/am507470f.

Lee, D.U., Park, M.G., Park, H.W., Seo, M.H., Ismayilov, V., Ahmed, R., Chen, Z., 2015c. Highly active Co-doped $LaMnO_3$ perovskite oxide and N-doped carbon nanotube hybrid bi-functional catalyst for rechargeable zinc–air batteries. Electrochem. Commun. 60, 38–41. https://doi.org/10.1016/j.elecom.2015.08.001.

Leng, M., Huang, X., Xiao, W., Ding, J., Liu, B., Du, Y., 2017. Nano Energy Enhanced oxygen evolution reaction by Co-O-C bonds in rationally designed Co_3O_4/graphene nanocomposites. Nano Energy 33, 445–452. https://doi.org/10.1016/j.nanoen.2017.01.061.

Leyva-García, S., Morallón, E., Cazorla-Amorós, D., Béguin, F., Lozano-Castelló, D., 2014. New insights on electrochemical hydrogen storage in nanoporous carbons by in situ Raman spectroscopy. Carbon 69, 401–408. https://doi.org/10.1016/j.carbon.2013.12.042.

Li, Y., Lu, J., 2017. Metal-air batteries: will they Be the future electrochemical energy storage device of choice? ACS Energy Lett. 2, 1370–1377. https://doi.org/10.1021/acsenergylett.7b00119.

Li, Q., He, R., Jensen, J.O., Bjerrum, N.J., 2003. Approaches and recent development of polymer electrolyte membranes for fuel cells operating above 100 °C. Chem. Mater. 15, 4896–4915. https://doi.org/10.1021/cm0310519.

Li, C., Han, X., Cheng, F., Hu, Y., Chen, C., Chen, J., 2015a. Phase and composition controllable synthesis of cobalt manganese spinel nanoparticles towards efficient oxygen electrocatalysis. Nat. Commun. 6, 1–8. https://doi.org/10.1038/ncomms8345.

Li, M., Xiong, Y., Liu, X., Bo, X., Zhang, Y., Han, C., Guo, L., 2015b. Facile synthesis of electrospun MFe_2O_4 (M = Co, Ni, Cu, Mn) spinel nanofibers with excellent electrocatalytic properties for oxygen evolution and hydrogen peroxide reduction. Nanoscale 7, 8920–8930. https://doi.org/10.1039/c4nr07243j.

Li, T., Liu, J., Jin, X., Wang, F., Song, Y., 2016a. Composition-dependent electro-catalytic activities of covalent carbon-$LaMnO_3$ hybrids as synergistic catalysts for oxygen reduction reaction. Electrochim. Acta 198, 115–126. https://doi.org/10.1016/j.electacta.2016.02.027.

Li, G., Liu, C., Chen, S., Hao, C., Cheng, G., Xie, Y., 2016b. Promotion of oxygen reduction performance by Fe_3O_4 nanoparticles support nitrogen-doped three dimensional meso/macroporous carbon based electrocatalyst. Int. J. Hydrogen Energy 42, 4133–4145. https://doi.org/10.1016/j.ijhydene.2016.10.081.

Li, R., Zhou, D., Luo, J., Xu, W., Li, J., Li, S., Cheng, P., 2017. The urchin-like sphere arrays Co_3O_4 as a bifunctional catalyst for hydrogen evolution reaction and oxygen evolution reaction. J. Power Sources 341, 250–256. https://doi.org/10.1016/j.jpowsour.2016.10.096.

Li, C., Yu, Z., Liu, H., Chen, K., 2018. High surface area $LaMnO_3$ nanoparticles enhancing electrochemical catalytic activity for rechargeable lithium-air batteries. J. Phys. Chem. Solid. 113, 151–156. https://doi.org/10.1016/j.jpcs.2017.10.039.

Li, M., Lu, M., Yang, J., Xiao, J., Han, L., Zhang, Y., Bo, X., 2019. Facile design of ultrafine $CuFe_2O_4$ nanocrystallines coupled porous carbon nanowires: highly effective electrocatalysts for hydrogen peroxide reduction and the oxygen evolution reaction. J. Alloys Compd. 809, 151766 https://doi.org/10.1016/j.jallcom.2019.151766.

Liang, Y., Li, Y., Wang, H., Zhou, J., Wang, J., Regier, T., Dai, H., 2011. Co_3O_4 nanocrystals on graphene as a synergistic catalyst for oxygen reduction reaction. Nat. Mater. 10, 780–786. https://doi.org/10.1038/nmat3087.

Lim, J., Hoffmann, M.R., 2019. Substrate oxidation enhances the electrochemical production of hydrogen peroxide. Chem. Eng. J. 374, 958–964. https://doi.org/10.1016/j.cej.2019.05.165.

Lim, D., Kong, H., Lim, C., Kim, N., Shim, S.E., Baeck, S.H., 2019. Spinel-type $NiCo_2O_4$ with abundant oxygen vacancies as a high-performance catalyst for the oxygen reduction reaction. Int. J. Hydrogen Energy 44, 23775–23783. https://doi.org/10.1016/j.ijhydene.2019.07.091.

Liu, J., Jin, X., Song, W., Wang, F., Wang, N., Song, Y., 2014. Facile preparation of modified carbon black-$LaMnO_3$ hybrids and the effect of covalent coupling on the catalytic activity for oxygen reduction reaction. Chin. J. Catal. 35, 1173–1188. https://doi.org/10.1016/S1872-2067(14)60066-8.

Liu, J., Jiang, L., Zhang, T., Jin, J., Yuan, L., Sun, G., 2016a. Activating Mn_3O_4 by morphology tailoring for oxygen reduction reaction. Electrochim. Acta 205, 38–44. https://doi.org/10.1016/j.electacta.2016.04.103.

Liu, G., Wang, K., Gao, X., He, D., Li, J., 2016b. Fabrication of mesoporous $NiFe_2O_4$ nanorods as efficient oxygen evolution catalyst for water splitting. Electrochim. Acta 211, 871–878. https://doi.org/10.1016/j.electacta.2016.06.113.

Liu, K., Li, J., Wang, Q., Wang, X., Qian, D., Jiang, J., Li, J., Chen, Z., 2017. Designed synthesis of $LaCoO_3$/N-doped reduced graphene oxide nanohybrid as an efficient bifunctional electrocatalyst for ORR and OER in alkaline medium. J. Alloys Compd. 725, 260–269. https://doi.org/10.1016/j.jallcom.2017.07.178.

Liu, X., Gong, H., Wang, T., Guo, H., Song, L., Xia, W., Gao, B., Jiang, Z., Feng, L., He, J., 2018. Cobalt-doped perovskite-type oxide $LaMnO_3$ as bifunctional oxygen catalysts for hybrid lithium-oxygen batteries. Chem. Asian J. 13, 528–535. https://doi.org/10.1002/asia.201701561.

Liu, J., Bao, H., Zhang, B., Hua, Q., Shang, M., Wang, J., Jiang, L., 2019a. Geometric occupancy and oxidation state requirements of cations in cobalt oxides for oxygen reduction reaction. ACS Appl. Mater. Interfaces 11, 12525–12534. https://doi.org/10.1021/acsami.9b00481.

Liu, G., Wang, B., Ding, P., Ye, Y., Wei, W., Zhu, W., Xu, L., Xia, J., Li, H., 2019b. Reactable ionic liquid in situ-induced synthesis of Fe_3O_4 nanoparticles modified N-doped hollow porous carbon microtubes for boosting multifunctional electrocatalytic activity. J. Alloys Compd. 797, 849–858. https://doi.org/10.1016/j.jallcom.2019.04.284.

Liu, Y., Liu, P., Qin, W., Wu, X., Yang, G., 2019c. Laser modification-induced $NiCo_2O_{4-\delta}$ with high exterior Ni^{3+}/Ni^{2+} ratio and substantial oxygen vacancies for electrocatalysis. Electrochim. Acta 297, 623–632. https://doi.org/10.1016/j.electacta.2018.11.111.

Liu, X.M., Cui, X., Dastafkan, K., Wang, H.F., Tang, C., Zhao, C., Chen, A., He, C., Han, M., Zhang, Q., 2020a. Recent advances in spinel-type electrocatalysts for bifunctional oxygen reduction and oxygen evolution reactions. J. Energy Chem. 53, 290–302. https://doi.org/10.1016/j.jechem.2020.04.012.

Liu, Y., Yang, L., Xie, B., Zhao, N., Yang, L., Zhan, F., Pan, Q., Han, J., Wang, X., Liu, J., Li, J., Yang, Y., 2020b. Ultrathin Co_3O_4 nanosheet clusters anchored on nitrogen doped carbon nanotubes/3D graphene as binder-free cathodes for Al-air battery. Chem. Eng. J. 381, 122681 https://doi.org/10.1016/j.cej.2019.122681.

Liu, W., Rao, D., Bao, J., Xu, L., Lei, Y., Li, H., 2021. Strong coupled spinel oxide with N-rGO for high-efficiency ORR/OER bifunctional electrocatalyst of Zn-air batteries. J. Energy Chem. 57, 428–435. https://doi.org/10.1016/j.jechem.2020.08.066.

Long, X., Yu, P., Zhang, N., Li, C., Feng, X., Ren, G., Zheng, S., Fu, J., Cheng, F., Liu, X., 2019. Direct spectroscopy for probing the critical role of partial covalency in oxygen reduction reaction for cobalt-manganese spinel oxides. Nanomaterials 9, 1–12. https://doi.org/10.3390/nano9040577.

Luo, Y., Alonso-Vante, N., 2015. The effect of support on advanced Pt-based cathodes towards the oxygen reduction reaction. State of the Art, Electrochim. Acta. 179, 108–118. https://doi.org/10.1016/j.electacta.2015.04.098.

Lv, Y., Li, Z., Yu, Y., Yin, J., Song, K., Yang, B., Yuan, L., Hu, X., 2019. Copper/cobalt-doped $LaMnO_3$ perovskite oxide as a bifunctional catalyst for rechargeable Li-O_2 batteries. J. Alloys Compd. 801, 19–26. https://doi.org/10.1016/j.jallcom.2019.06.114.

Lv, X., Liu, Y., Tian, W., Gao, L., Yuan, Z., 2020. Aluminum and phosphorus codoped " superaerophobic " Co_3O_4 microspheres for highly efficient electrochemical water splitting and Zn-air batteries. J. Energy Chem. 50, 324–331. https://doi.org/10.1016/j.jechem.2020.02.055.

Ma, Z., Zhang, Y., Liu, S., Xu, W., Wu, L., Hsieh, Y.C., Liu, P., Zhu, Y., Sasaki, K., Renner, J.N., Ayers, K.E., Adzic, R.R., Wang, J.X., 2018. Reaction mechanism for oxygen evolution on RuO_2, IrO_2, and RuO_2@IrO_2 core-shell nanocatalysts. J. Electroanal. Chem. 819, 296–305. https://doi.org/10.1016/j.jelechem.2017.10.062.

Majee, R., Chakraborty, S., Salunke, H.G., Bhattacharyya, S., 2018. Maneuvering the physical properties and spin states to enhance the activity of La–Sr–Co–Fe–O perovskite oxide nanoparticles in electrochemical water oxidation. ACS Appl. Energy Mater. 1 https://doi.org/10.1021/acsaem.8b00531 acsaem.8b00531.

Mathumba, P., Fernandes, D.M., Matos, R., Iwuoha, E.I., Freire, C., 2020. Metal oxide (Co_3O_4 and Mn_3O_4) impregnation into S, N-doped graphene for oxygen reduction reaction (ORR). Materials 13, 1562. https://doi.org/10.3390/ma13071562.

Matseke, M.S., Zheng, H., Wang, Y., 2020. The ultrasonication boosts the surface properties of $CoFe_2O_4$/C nanoparticles towards ORR in alkaline media. Appl. Surf. Sci. 516, 146105 https://doi.org/10.1016/j.apsusc.2020.146105.

Matsumoto, Y., Yoneyama, H., Tamura, H., 1977a. Influence of the nature of the conduction band of transition metal oxides on catalytic activity for oxygen reduction. J. Electroanal. Chem. Interfacial Electrochem. 83, 237–243. https://doi.org/10.1016/S0022-0728(77)80169-1.

Matsumoto, Y., Yoneyama, H., Tamura, H., 1977b. Catalytic activity for electrochemical reduction of oxygen of lanthanum nickel oxide and related oxides. J. Electroanal. Chem. Interfacial Electrochem. 79, 319–326. https://doi.org/10.1016/S0022-0728(77)80453-1.

Matsumoto, Y., Yoneyama, H., Tamura, H., 1978. MECHANISM OF OXYGEN REDUCTION AT A LaNiO3 ELECTRODE. Bull. Chem. Soc. Jpn. 51, 1927–1930. https://doi.org/10.1246/bcsj.51.1927.

Mattick, V.F., Jin, X., Yang, T., White, R.E., Huang, K., 2018. Unraveling oxygen electrocatalysis mechanisms on a thin-film oxygen-deficient perovskite $La_{0.6}Sr_{0.4}CoO_{3-\delta}$. ACS Appl. Energy Mater. 1, 3937–3946. https://doi.org/10.1021/acsaem.8b00669.

Mazloomi, K., Gomes, C., 2012. Hydrogen as an energy carrier: prospects and challenges. Renew. Sustain. Energy Rev. 16, 3024–3033. https://doi.org/10.1016/j.rser.2012.02.028.

Medford, A.J., Vojvodic, A., Hummelshøj, J.S., Voss, J., Abild-Pedersen, F., Studt, F., Bligaard, T., Nilsson, A., Nørskov, J.K., 2015. From the Sabatier principle to a predictive theory of transition-metal heterogeneous catalysis. J. Catal. 328, 36–42. https://doi.org/10.1016/j.jcat.2014.12.033.

Mefford, J.T., Rong, X., Abakumov, A.M., Hardin, W.G., Dai, S., Kolpak, A.M., Johnston, K.P., Stevenson, K.J., 2016. Water electrolysis on $La_{1-x}Sr_xCoO_{3-\delta}$ perovskite electrocatalysts. Nat. Commun. 7 https://doi.org/10.1038/ncomms11053.

Mefford, J.T., Kurilovich, A.A., Saunders, J., Hardin, W.G., Abakumov, A.M., Forslund, R.P., Bonnefont, A., Dai, S., Johnston, K.P., Stevenson, K.J., 2019. Decoupling the roles

of carbon and metal oxides on the electrocatalytic reduction of oxygen on $La_{1-x}Sr_xCoO_{3-\delta}$ perovskite composite electrodes. Phys. Chem. Chem. Phys. 21, 3327–3338. https://doi.org/10.1039/C8CP06268D.
Miao, H., Wu, X., Chen, B., Wang, Q., Wang, F., Wang, J., Zhang, C., Zhang, H., Yuan, J., Zhang, Q., 2020. A-site deficient/excessive effects of $LaMnO_3$ perovskite as bifunctional oxygen catalyst for zinc-air batteries. Electrochim. Acta 333, 135566. https://doi.org/10.1016/j.electacta.2019.135566.
Miyahara, Y., Miyazaki, K., Fukutsuka, T., Abe, T., 2014. Catalytic roles of perovskite oxides in electrochemical oxygen reactions in alkaline media. J. Electrochem. Soc. 161, F694. https://doi.org/10.1149/2.019406jes. –F697.
Mulder, K., Ferrer, D., van Lente, H., 2011. What is Sustainable Technology?: Perceptions, Paradoxes and Possibilites, first ed. Routledge. https://doi.org/10.4324/9781351278485.
Najam, T., Cai, X., Aslam, M.K., Tufail, M.K., Shah, S.S.A., 2020. Nano-engineered directed growth of Mn_3O_4 quasi-nanocubes on N-doped polyhedrons: efficient electrocatalyst for oxygen reduction reaction. Int. J. Hydrogen Energy 45, 12903–12910. https://doi.org/10.1016/j.ijhydene.2020.02.205.
Nguyen, T.D., Scherer, G.G., Xu, Z.J., 2016. A facile synthesis of size-controllable IrO_2 and RuO_2 nanoparticles for the oxygen evolution reaction. Electrocatalysis 7, 420–427. https://doi.org/10.1007/s12678-016-0321-2.
Ollo, K., Aliou Guillaume, P.L., Auguste, A.F.T., Quand-Meme, G.C., Honoré, K.K., Ouattara, L., 2015. Influence of various metallic oxides on the kinetic of the oxygen evolution reaction on platinum electrodes. J. Electrochem. Sci. Eng. 5, 79–91. https://doi.org/10.5599/jese.157.
Osgood, H., Devaguptapu, S.V., Xu, H., Cho, J., Wu, G., 2016. Transition metal (Fe, Co, Ni, and Mn) oxides for oxygen reduction and evolution bifunctional catalysts in alkaline media. Nano Today 11, 601–625. https://doi.org/10.1016/j.nantod.2016.09.001.
Pan, L., Zhu, G., 2016. Perovskite Materials - Synthesis, Characterisation, Properties, and Applications. InTechOpen, London. https://doi.org/10.5772/60469.
Pan, Z.F., An, L., Zhao, T.S., Tang, Z.K., 2018. Advances and challenges in alkaline anion exchange membrane fuel cells. Prog. Energy Combust. Sci. 66, 141–175. https://doi.org/10.1016/j.pecs.2018.01.001.
Park, H.W., Lee, D.U., Park, M.G., Ahmed, R., Seo, M.H., Nazar, L.F., Chen, Z., 2015. Perovskite-nitrogen-doped carbon nanotube composite as bifunctional catalysts for rechargeable lithium-air batteries. ChemSusChem 8, 1058–1065. https://doi.org/10.1002/cssc.201402986.
Pawar, S.M., Pawar, B.S., Babar, P.T., Ahmed, A.T.A., Chavan, H.S., Jo, Y., Cho, S., Kim, J., Hou, B., Inamdar, A.I., Cha, S.N., Kim, J.H., Kim, T.G., Kim, H., Im, H., 2019. Nanoporous $CuCo_2O_4$ nanosheets as a highly efficient bifunctional electrode for supercapacitors and water oxidation catalysis. Appl. Surf. Sci. 470, 360–367. https://doi.org/10.1016/j.apsusc.2018.11.151.
Pennycook, S.J., Guan, M., Yang, J., Tsai, M.-C., Hu, Y., Gong, M., Zhou, W., Zhou, J., Hwang, B.-J., Dai, H., Wang, D.-Y., Lin, M.-C., Zhang, B., 2014. Nanoscale nickel oxide/nickel heterostructures for active hydrogen evolution electrocatalysis. Nat. Commun. 5, 1–6. https://doi.org/10.1038/ncomms5695.
Perry, K., 2020. Britain to ban the Sale of New Petrol and Diesel cars Just 10 Years from Now. Mirror.
Poux, T., Napolskiy, F.S., Dintzer, T., Kéranguéven, G., Istomin, S.Y., Tsirlina, G.A., Antipov, E.V., Savinova, E.R., 2012. Dual role of carbon in the catalytic layers of perovskite/carbon composites for the electrocatalytic oxygen reduction reaction. Catal. Today 189, 83–92. https://doi.org/10.1016/j.cattod.2012.04.046.
Qian, J., Li, J., Xia, B., Zhang, J., Zhang, Z., Guan, C., Gao, D., Huang, W., 2021. Multi-stability modulating of alkaline-earth metal doped $LaCoO_3$ for rechargeable Zn-air batteries. Energy Storage Mater. 42, 470–476. https://doi.org/10.1016/j.ensm.2021.08.007.
Quílez-Bermejo, J., Morallón, E., Cazorla-Amorós, D., 2020. Metal-free heteroatom-doped carbon-based catalysts for ORR. A critical assessment about the role of heteroatoms. Carbon 165, 434–454. https://doi.org/10.1016/j.carbon.2020.04.068.
Quaino, P., Juarez, F., Santos, E., Schmickler, W., 2014. Volcano plots in hydrogen electrocatalysis – uses and abuses. Beilstein J. Nanotechnol. 5, 846–854. https://doi.org/10.3762/bjnano.5.96.
Rado, A., Dryga, A., Hawe, Ł., Dariusz, Ł., 2017. Materials Characterization Structure and optical properties of Fe_3O_4 nanoparticles synthesized by co-precipitation method with di ff erent organic modi fi ers. Mater. Char. 131, 148–156. https://doi.org/10.1016/j.matchar.2017.06.034.
Ramaswamy, N., Mukerjee, S., 2012. Fundamental mechanistic understanding of electrocatalysis of oxygen reduction on Pt and non-Pt surfaces: acid versus alkaline media. Adv. Phys. Chem. 2012, 491604 https://doi.org/10.1155/2012/491604.
Rao, C.N.R., 2003. Perovskites. In: Meyers, R.A. (Ed.), Encyclopedia of Physical Science and Technology, third ed. Academic Press, New York, pp. 707–714. https://doi.org/10.1016/B0-12-227410-5/00554-8.
Rebekah, A., Ashok Kumar, E., Viswanathan, C., Ponpandian, N., 2020. Effect of cation substitution in $MnCo_2O_4$ spinel anchored over rGO for enhancing the electrocatalytic activity towards oxygen evolution reaction (OER). Int. J. Hydrogen Energy 45, 6391–6403. https://doi.org/10.1016/j.ijhydene.2019.12.164.
Reddy, K.P., Jain, R., Ghosalya, M.K., Gopinath, C.S., 2017. Metallic cobalt to spinel Co_3O_4 - electronic structure evolution by near-ambient pressure photoelectron spectroscopy. J. Phys. Chem. 121, 21472–21481. https://doi.org/10.1021/acs.jpcc.7b06661.
Reier, T., Oezaslan, M., Strasser, P., 2012. Electrocatalytic oxygen evolution reaction (OER) on Ru, Ir, and Pt catalysts: a comparative study of nanoparticles and bulk materials. ACS Catal. 2, 1765–1772. https://doi.org/10.1021/cs3003098.
Retuerto, M., Pereira, A.G., Pérez-Alonso, F.J., Peña, M.A., Fierro, J.L.G., Alonso, J.A., Fernández-Díaz, M.T., Pascual, L., Rojas, S., 2017. Structural effects of $LaNiO_3$ as electrocatalyst for the oxygen reduction reaction. Appl. Catal. B Environ. 203, 363–371. https://doi.org/10.1016/j.apcatb.2016.10.016.
Risch, M., 2017. Perovskite electrocatalysts for the Oxygen reduction reaction in alkaline media. Catalysts 7, 25–28. https://doi.org/10.3390/catal7050154.
Rong, X., Parolin, J., Kolpak, A.M., 2016. A fundamental relationship between reaction mechanism and stability in metal oxide catalysts for oxygen evolution. ACS Catal. 6, 1153–1158. https://doi.org/10.1021/acscatal.5b02432.
Ryabova, A.S., Bonnefont, A., Simonov, P.A., Dintzer, T., Ulhaq-Bouillet, C., Bogdanova, Y.G., Tsirlina, G.A., Savinova, E.R., 2017. Further insights into the role of carbon in manganese oxide/carbon composites in the oxygen reduction reaction in alkaline media. Electrochim. Acta 246, 643–653. https://doi.org/10.1016/j.electacta.2017.06.017.
Safakas, A., Bampos, G., Bebelis, S., 2019. Oxygen reduction reaction on $La_{0.8}Sr_{0.2}Co_xFe_{1-x}O_{3-\delta}$ perovskite/carbon black electrocatalysts in alkaline medium. Appl. Catal. B Environ. 244, 225–232. https://doi.org/10.1016/j.apcatb.2018.11.015.
Samanta, A., Raj, C.R., 2019. A new approach for the synthesis of electrocatalytically active $CoFe_2O_4$ catalyst for oxygen reduction reaction. J. Electroanal. Chem. 847, 113183 https://doi.org/10.1016/j.jelechem.2019.05.065.
Serov, A., Andersen, N.I., Roy, A.J., Matanovic, I., Artyushkova, K., Atanassov, P., 2015. $CuCo_2O_4$ ORR/OER Bi-functional catalyst: influence of synthetic approach on performance. J. Electrochem. Soc. 162, F449–F454. https://doi.org/10.1149/2.0921504jes.
Shao, M., Chang, Q., Dodelet, J.-P., Chenitz, R., 2016. Recent advances in electrocatalysts for oxygen reduction reaction. Chem. Rev. 116, 3594–3657. https://doi.org/10.1021/acs.chemrev.5b00462.
Sheng, W., Myint, M., Chen, J.G., Yan, Y., 2013. Correlating the hydrogen evolution reaction activity in alkaline electrolytes with the hydrogen binding energy on monometallic surfaces. Energy Environ. Sci. 6, 1509–1512. https://doi.org/10.1039/c3ee00045a.
Shenghai, C., Liping, S., Fanhao, K., Lihua, H., Hui, Z., 2019. Carbon-coated $MnCo_2O_4$ nanowire as bifunctional oxygen catalysts for rechargeable Zn-air batteries. J. Power Sources 430, 25–31. https://doi.org/10.1016/j.jpowsour.2019.05.029.
Shi, C., Ullah, S., Li, K., Wang, W., Zhang, R., Pan, L., Zhang, X., Zou, J.J., 2020. Low-temperature synthesis of ultrasmall spinel $Mn_xCo_{3-x}O_4$ nanoparticles for efficient oxygen reduction. Chin. J. Catal. 41, 1818–1825. https://doi.org/10.1016/S1872-2067(20)63624-5.
Shinagawa, T., Garcia-Esparza, A.T., Takanabe, K., 2015. Insight on Tafel slopes from a microkinetic analysis of aqueous electrocatalysis for energy conversion. Sci. Rep. 5, 13801 https://doi.org/10.1038/srep13801.
Shirvanian, P., van Berkel, F., 2020. Novel components in proton exchange membrane water electrolyzers (PEMWE): status, challenges and future needs. Electrochem. Commun. 114, 106704 https://doi.org/10.1016/j.elecom.2020.106704.
Shui, Z., Zhao, W., Xiao, H., Zhu, L., Liu, Y., Deng, X., Chen, X., 2022. Controllable porous perovskite with three-dimensional ordered structure as an efficient oxygen reduction reaction electrocatalyst for flexible aluminum-air battery. J. Power Sources 523, 231028. https://doi.org/10.1016/j.jpowsour.2022.231028.
Si, C., Zhang, Y., Zhang, C., Gao, H., Ma, W., Lv, L., Zhang, Z., 2017. Mesoporous nanostructured spinel-type MFe_2O_4 (M = Co, Mn, Ni) oxides as efficient bi-functional electrocatalysts towards oxygen reduction and oxygen evolution. Electrochim. Acta 245, 829–838. https://doi.org/10.1016/j.electacta.2017.06.029.
Silva, V.D., Ferreira, L.S., Simões, T.A., Medeiros, E.S., Macedo, D.A., 2019. 1D hollow MFe_2O_4 (M = Cu, Co, Ni) fibers by Solution Blow Spinning for oxygen evolution reaction. J. Colloid Interface Sci. 540, 59–65. https://doi.org/10.1016/j.jcis.2019.01.003.
Stacy, J., Regmi, Y.N., Leonard, B., Fan, M., 2017. The recent progress and future of oxygen reduction reaction catalysis: a review. Renew. Sustain. Energy Rev. 69, 401–414. https://doi.org/10.1016/j.rser.2016.09.135.
Stoerzinger, K.A., Lü, W., Li, C., Ariando, Venkatesan, T., Shao-Horn, Y., 2015. Highly active epitaxial $La_{(1-x)}Sr_xMnO_3$ surfaces for the oxygen reduction reaction: role of charge transfer. J. Phys. Chem. Lett. 6, 1435–1440. https://doi.org/10.1021/acs.jpclett.5b00439.
Su, Y., Liu, H., Li, C., Liu, J., Song, Y., Wang, F., 2019. Hydrothermal-assisted defect engineering in spinel Co_3O_4 nanostructures as bifunctional catalysts for oxygen electrode. J. Alloys Compd. 799, 160–168. https://doi.org/10.1016/j.jallcom.2019.05.331.
Sun, J., Du, L., Sun, B., Han, G., Ma, Y., Wang, J., Huo, H., Du, C., Yin, G., 2020. Bifunctional $LaMn_{0.3}Co_{0.7}O_3$ perovskite oxide catalyst for oxygen reduction and evolution reactions: the optimized egElectronic structures by manganese dopant. ACS Appl. Mater. Interfaces 12, 24717–24725. https://doi.org/10.1021/acsami.0c03983.
Sun, J., Du, L., Sun, B., Han, G., Ma, Y., Wang, J., Huo, H., Zuo, P., Du, C., Yin, G., 2021. A bifunctional perovskite oxide catalyst: the triggered oxygen reduction/evolution electrocatalysis by moderated Mn-Ni co-doping. J. Energy Chem. 54, 217–224. https://doi.org/10.1016/j.jechem.2020.05.064.
Sunarso, J., Torriero, A.A.J., Zhou, W., Howlett, P.C., Forsyth, M., 2012. Oxygen reduction reaction activity of La-based perovskite oxides in alkaline medium: a thin-film rotating ring-disk electrode study. J. Phys. Chem. C 116, 5827–5834. https://doi.org/10.1021/jp211946n.
Suntivich, J., Gasteiger, H.A., Yabuuchi, N., Nakanishi, H., Goodenough, J.B., Shao-Horn, Y., 2011a. Design principles for oxygen-reduction activity on perovskite oxide catalysts for fuel cells and metal–air batteries. Nat. Chem. 3, 546–550. https://doi.org/10.1038/nchem.1069.
Suntivich, J., May, K.J., Gasteiger, H.A., Goodenough, J.B., Shao-Horn, Y., 2011b. A perovskite oxide optimized for oxygen evolution catalysis from molecular orbital principles. Science 334, 1383–1385. https://doi.org/10.1126/science.1212858.

Tejuca, L.G., Fierro, J.L.G., 1989. Structure and reactivity of perovskite-type oxides. Adv. Catal. 36, 237–328.
Thomas, S., Zalbowitz, M., 1999. Fuel Cells: Green Power. Los Alamos National Laboratory, USA, pp. 1–36.
Tomon, C., Krittayavathananon, A., Sarawutanukul, S., 2021. Enhancing bifunctional electrocatalysts of hollow Co_3O_4 nanorods with oxygen vacancies towards ORR and OER for Li–O_2 batteries. Electrochim. Acta 367, 137490. https://doi.org/10.1016/j.electacta.2020.137490.
Trasatti, S., 1972. Work function, electronegativity, and electrochemical behaviour of metals. J. Electroanal. Chem. Interfacial Electrochem. 39, 163–184. https://doi.org/10.1016/S0022-0728(72)80485-6.
UNFCC, 2008. Kyoto Protocol Reference Manual on Accounting of Emissions and Assigned Amount, 92-9219-055-5. Available online: https://unfccc.int/resource/docs/publications/08_unfccc_kp_ref_manual.pdf.
UNFCC. Paris agreement (annex to decision 1/CP,21, 2015 document FCCC/CP/201510/Add.1 Paris: united Nations). Available online: https://unfccc.int/resource/docs/2015/cop21/eng/10a01.pdf.
Vazhayil, A., Thomas, J., Thomas, N., 2022. Cobalt doping in $LaMnO_3$ perovskite catalysts – B site optimization by solution combustion for oxygen evolution reaction. J. Electroanal. Chem. 918, 116426 https://doi.org/10.1016/j.jelechem.2022.116426.
Vignesh, A., Prabu, M., Shanmugam, S., 2016. Porous $LaCo_{1-x}Ni_xO_{3-\delta}$ nanostructures as an efficient electrocatalyst for water oxidation and for a zinc–air battery. ACS Appl. Mater. Interfaces 8, 6019–6031. https://doi.org/10.1021/acsami.5b11840.
Wang, Y., Chen, K.S., Mishler, J., Cho, S.C., Adroher, X.C., 2011. A review of polymer electrolyte membrane fuel cells: technology, applications, and needs on fundamental research. Appl. Energy 88, 981–1007. https://doi.org/10.1016/j.apenergy.2010.09.030.
Wang, M., Huang, J., Wang, M., Zhang, D., Zhang, W., Li, W., Chen, J., 2013. Electrochemistry Communications Co_3O_4 nanorods decorated reduced graphene oxide composite for oxygen reduction reaction in alkaline electrolyte. Electrochem. Commun. 34, 299–303. https://doi.org/10.1016/j.elecom.2013.07.017.
Wang, Z., You, Y., Yuan, J., Yin, Y.X., Li, Y.T., Xin, S., Zhang, D., 2016a. Nickel-doped $La_{0.8}Sr_{0.2}Mn_{1-x}Ni_xO_3$ nanoparticles containing abundant oxygen vacancies as an optimized bifunctional catalyst for oxygen cathode in rechargeable lithium-air batteries. ACS Appl. Mater. Interfaces 8, 6520–6528. https://doi.org/10.1021/acsami.6b00296.
Wang, J., Fu, Y., Xu, Y., Wu, J., Tian, J.H., Yang, R., 2016b. Hierarchical $NiCo_2O_4$ hollow nanospheres as high efficient bi-functional catalysts for oxygen reduction and evolution reactions. Int. J. Hydrogen Energy 41, 8847–8854. https://doi.org/10.1016/j.ijhydene.2016.03.154.
Wang, P.X., Shao, L., Zhang, N.Q., Sun, K.N., 2016c. Mesoporous $CuCo_2O_4$ nanoparticles as an efficient cathode catalyst for Li-O_2 batteries. J. Power Sources 325, 506–512. https://doi.org/10.1016/j.jpowsour.2016.06.065.
Wang, B., Xu, L., Liu, G., Zhang, P., Zhu, W., Xia, J., Li, H., 2017a. Biomass willow catkin-derived Co_3O_4/N-doped hollow hierarchical porous carbon microtubes as an effective tri-functional electrocatalyst. J. Mater. Chem. A. 5, 20170–20179. https://doi.org/10.1039/C7TA05002J.
Wang, Q., Qiu, X., Hu, W., Huang, Y., 2017b. Facile synthesis of three-dimensional porous nitrogen doped carbon supported Co_3O_4 for oxygen reduction reaction and oxygen evolution reaction. Mater. Lett. 190, 169–172. https://doi.org/10.1016/j.matlet.2016.12.117.
Wang, H., Liu, R., Li, Y., Lü, X., Wang, Q., Zhao, S., Yuan, K., Cui, Z., Li, X., Xin, S., Zhang, R., Lei, M., Lin, Z., 2018. Durable and efficient hollow porous oxide spinel microspheres for oxygen reduction. Joule 2, 337–348. https://doi.org/10.1016/j.joule.2017.11.016.
Wang, H., Xu, W., Richins, S., Liaw, K., Yan, L., Zhou, M., Luo, H., 2019. Polymer-assisted approach to $LaCo_{1-x}Ni_xO_3$ network nanostructures as bifunctional oxygen electrocatalysts. Electrochim. Acta 296, 945–953. https://doi.org/10.1016/j.electacta.2018.11.075.
Wang, H., Liu, C., Yang, X., Gu, J., Niu, M., Yang, L., Bai, Z., 2022. In situ synthesis of $CoFe_2O_4$ nanoparticles embedded in N-doped carbon nanotubes for efficient electrocatalytic oxygen reduction reaction. Int. J. Hydrogen Energy 47, 6059–6066. https://doi.org/10.1016/j.ijhydene.2021.11.220.
Wehrmann, B., 2020. Germany remains odd one out as more and more countries announce combustion engine bans. Clean Energy Wire, Journal. Energy Transit. https://www.cleanenergywire.org/news/germany-remains-odd-one-out-more-and-more-countries-announce-combustion-engine-bans.
Wei, C., Feng, Z., Scherer, G.G., Barber, J., Shao-Horn, Y., Xu, Z.J., 2017. Cations in octahedral sites: a descriptor for oxygen electrocatalysis on transition-metal spinels. Adv. Mater. 29, 1–8. https://doi.org/10.1002/adma.201606800.
Wei, J., Zhou, M., Long, A., Xue, Y., Liao, H., Wei, C., Xu, Z.J., 2018. Heterostructured electrocatalysts for hydrogen evolution reaction under alkaline conditions. Nano-Micro Lett. 10, 1–15. https://doi.org/10.1007/s40820-018-0229-x.
Wei, B., Wu, J., Mei, G., Qi, Z., Hu, W., Wang, Z., 2019. $NiCo_2O_4$ nanowire arrays rich in oxygen deficiencies for hydrogen evolution reaction. Int. J. Hydrogen Energy 44, 6612–6617. https://doi.org/10.1016/j.ijhydene.2019.01.183.
Wei, M., Han, Y., Liu, Y., Su, B., Yang, H., Lei, Z., 2020. Green preparation of Fe_3O_4 coral-like nanomaterials with outstanding magnetic and OER properties. J. Alloys Compd. 831, 154702 https://doi.org/10.1016/j.jallcom.2020.154702.
Winter, M., Brodd, R.J., 2004. What are batteries, fuel cells, and supercapacitors? Chem. Rev. 104, 4245–4269. https://doi.org/10.1021/cr020730k.
Wu, J., Yang, H., 2013. Platinum-based oxygen reduction electrocatalysts. Acc. Chem. Res. 46, 1848–1857. https://doi.org/10.1021/ar300359w.
Wu, K., Shen, D., Meng, Q., Wang, J., 2018a. Octahedral Co_3O_4 particles with high electrochemical surface area as electrocatalyst for water splitting. Electrochim. Acta 288, 82–90. https://doi.org/10.1016/j.electacta.2018.08.067.
Wu, X., Niu, Y., Feng, B., Yu, Y., Huang, X., Zhong, C., Hu, W., Li, C.M., 2018b. Mesoporous hollow nitrogen-doped carbon nanospheres with embedded $MnFe_2O_4$/Fe hybrid nanoparticles as efficient bifunctional oxygen electrocatalysts in alkaline media. ACS Appl. Mater. Interfaces 10, 20440–20447. https://doi.org/10.1021/acsami.8b04012.
Wu, F., Feng, B., Li, W., Liu, H., Mei, Y., Hu, W., 2019. Efficient oxygen reduction electrocatalysis on Mn_3O_4 nanoparticles decorated N-doped carbon with hierarchical porosity and abundant active sites. Int. J. Hydrogen Energy 44, 26387–26395. https://doi.org/10.1016/j.ijhydene.2019.08.139.
Xu, G.R., Hui, J.J., Huang, T., Chen, Y., Lee, J.M., 2015a. Platinum nanocuboids supported on reduced graphene oxide as efficient electrocatalyst for the hydrogen evolution reaction. J. Power Sources 285, 393–399. https://doi.org/10.1016/j.jpowsour.2015.03.131.
Xu, Y., Bian, W., Wu, J., Tian, J.H., Yang, R., 2015b. Preparation and electrocatalytic activity of 3D hierarchical porous spinel $CoFe_2O_4$ hollow nanospheres as efficient catalyst for Oxygen Reduction Reaction and Oxygen Evolution Reaction. Electrochim. Acta 151, 276–283. https://doi.org/10.1016/j.electacta.2014.11.042.
Xu, Y., Tsou, A., Fu, Y., Wang, J., Tian, J.-H., Yang, R., 2015c. Carbon-coated perovskite BaMnO3 porous nanorods with enhanced electrocatalytic perporites for oxygen reduction and oxygen evolution. Electrochim. Acta 174, 551–556. https://doi.org/10.1016/j.electacta.2015.05.184.
Xu, L., Jiang, Q., Xiao, Z., Li, X., Huo, J., Wang, S., Dai, L., 2016. Oxygen vacancies plasma-engraved Co_3O_4 nanosheets with oxygen vacancies and high surface area for the oxygen evolution reaction. Angew. Chem. 5277–5281. https://doi.org/10.1002/anie.201600687.
Xue, Y., Miao, H., Sun, S., Wang, Q., Li, S., Liu, Z., 2017. $(La_{1-x}Sr_x)_{0.98}MnO_3$ perovskite with A-site deficiencies toward oxygen reduction reaction in aluminum-air batteries. J. Power Sources 342, 192–201. https://doi.org/10.1016/j.jpowsour.2016.12.065.
Yang, J., Sun, H., Park, G., An, J., Shim, J., 2018. Synthesis of highly porous $LaCoO_3$ catalyst by Nanocasting and its performance for oxygen reduction and evolution reactions in alkaline solution. J. Electroceram. 41, 80–87. https://doi.org/10.1007/s10832-018-0165-7.
Yang, Y., Xiong, Y., Holtz, M.E., Feng, X., Zeng, R., Chen, G., DiSalvo, F.J., Muller, D.A., Abruña, H.D., 2019. Octahedral spinel electrocatalysts for alkaline fuel cells. Proc. Natl. Acad. Sci. U.S.A. 116, 24425–24432. https://doi.org/10.1073/pnas.1906570116.
Yao, L., Zhong, H., Deng, C., Li, X., Zhang, H., 2016. Template-assisted synthesis of hierarchically porous Co_3O_4 with enhanced oxygen evolution activity. J. Energy Chem. 25, 153–157. https://doi.org/10.1016/j.jechem.2015.11.013.
Yoo, J.S., Rong, X., Liu, Y., Kolpak, A.M., 2018. Role of lattice oxygen participation in understanding trends in the oxygen evolution reaction on perovskites. ACS Catal. 8, 4628–4636. https://doi.org/10.1021/acscatal.8b00612.
Yuan, S., Fan, Y., Zhang, Y., Tong, M., Liao, P., 2011. Pd-catalytic in situ generation of H_2O_2 from H_2 and O_2 produced by water electrolysis for the efficient electro-fenton degradation of Rhodamine B. Environ. Sci. Technol. 45, 8514–8520. https://doi.org/10.1021/es2022939.
Yuan, R., He, Y., He, W., Ni, M., Leung, M.K.H., 2019a. $La_{0.8}Sr_{0.2}MnO_3$ based perovskite with A-site deficiencies as high performance bifunctional electrocatalyst for oxygen reduction and evolution reaction in alkaline. Energy Proc. 158, 5804–5810. https://doi.org/10.1016/j.egypro.2019.01.548.
Yuan, F., Cheng, X., Wang, M., Ni, Y., 2019b. Controlled synthesis of tubular ferrite MFe_2O_4 (M = Fe, Co, Ni) microstructures with efficiently electrocatalytic activity for water splitting. Electrochim. Acta 324, 134883. https://doi.org/10.1016/j.electacta.2019.134883.
Zadick, A., Dubau, L., Sergent, N., Berthomé, G., Chatenet, M., 2015. Huge instability of Pt/C catalysts in alkaline medium. ACS Catal. 5, 4819–4824. https://doi.org/10.1021/acscatal.5b01037.
Zhang, J., 2008. PEM Fuel cell Electrocatalysts and catalyst Layers: Fundamentals and Applications. https://doi.org/10.1007/978-1-84800-936-3.
Zhang, H., Zhao, Y., Zhang, Y., Zhang, M., Cheng, M., Yu, J., 2019. Fe_3O_4 encapsulated in porous carbon nanobowls as efficient oxygen reduction reaction catalyst for Zn-air batteries. Chem. Eng. J. 375, 122058 https://doi.org/10.1016/j.cej.2019.122058.
Zhang, W., Cui, L., Liu, J., 2020a. Recent advances in cobalt-based electrocatalysts for hydrogen and oxygen evolution reactions. J. Alloys Compd. 821, 153542 https://doi.org/10.1016/j.jallcom.2019.153542.
Zhang, Q., Han, W., Xu, Z., Li, Y., Chen, L., Bai, Z., Yang, L., Wang, X., 2020b. Hollow waxberry-like cobalt–nickel oxide/S,N-codoped carbon nanospheres as a trifunctional electrocatalyst for OER, ORR, and HER. RSC Adv. 10, 27788–27793. https://doi.org/10.1039/D0RA03222K.
Zhang, Y., Ullah, S., Zhang, R., Pan, L., Zhang, X., 2020c. Manipulating electronic delocalization of Mn_3O_4 by manganese defects for oxygen reduction reaction. Appl. Catal. B Environ. 277, 119247 https://doi.org/10.1016/j.apcatb.2020.119247.
Zhang, X., Guo, B., Lin, Z., Dong, B., Chen, Q., Dong, Y., Yang, M., Wang, L., 2020d. In situ electro-reduction to modulate the surface electronic structure of Fe_3O_4 for enhancing oxygen evolution reaction. Int. J. Hydrogen Energy 45, 15476–15482. https://doi.org/10.1016/j.ijhydene.2020.04.047.
Zhang, Y., Wang, Y., Huang, J., Han, C., Zang, J., 2020e. Mn_3O_4 nanosheets coated on carbon nanotubes as efficient electrocatalysts for oxygen reduction reaction. Int. J. Hydrogen Energy 45, 6529–6537. https://doi.org/10.1016/j.ijhydene.2019.12.216.
Zhao, Y., Hang, Y., Zhang, Y., Wang, Z., Yao, Y., He, X., Zhang, C., Zhang, D., 2017a. Strontium-doped perovskite oxide $La_{1-x}Sr_xMnO_3$ (x = 0, 0.2, 0.6) as a highly efficient electrocatalyst for nonaqueous Li-O_2 batteries. Electrochim. Acta 232, 296–302. https://doi.org/10.1016/j.electacta.2017.02.155.

Zhao, S., Rasimick, B., Mustain, W., Xu, H., 2017b. Highly durable and active Co_3O_4 nanocrystals supported on carbon nanotubes as bifunctional electrocatalysts in alkaline media. Applied Catal. B, Environ. 203, 138–145. https://doi.org/10.1016/j.apcatb.2016.09.048.

Zhao, Y., Liu, T., Shi, Q., Yang, Q., Li, C., Zhang, D., Zhang, C., 2018. Perovskite oxides $La_{0.4}Sr_{0.6}Co_xMn_{1-x}O_3$ (x = 0, 0.2, 0.4) as an effective electrocatalyst for lithium—air batteries. Green Energy Environ 3, 78–85. https://doi.org/10.1016/j.gee.2017.12.001.

Zhou, J., Song, H., Ma, L., Chen, X., 2011. Magnetite/graphene nanosheet composites: interfacial interaction and its impact on the durable high-rate performance in lithium-ion batteries. RSC Adv. 1, 782. https://doi.org/10.1039/c1ra00402f.

Zhu, H., Zhang, S., Huang, Y.X., Wu, L., Sun, S., 2013. Monodisperse $M_xFe_{3-x}O_4$ (M = Fe, Cu, Co, Mn) nanoparticles and their electrocatalysis for oxygen reduction reaction. Nano Lett. 13, 2947–2951. https://doi.org/10.1021/nl401325u.

Zhu, L., Ran, R., Tadé, M., Wang, W., Shao, Z., 2016. Perovskite materials in energy storage and conversion, Asia-Pacific. J. Chem. Eng. 11, 338–369. https://doi.org/10.1002/apj.2000.

Zhu, Y., Zhou, W., Shao, Z., 2017. Perovskite/carbon composites: applications in oxygen electrocatalysis. Small 13, 1603793. https://doi.org/10.1002/smll.201603793.

Zhuang, S., Wang, Z., He, J., Jia, D., Wang, Q., Lu, M., Tu, F., 2021. Perovskite $La_{0.5}Ca_{0.5}CoO_{3-\delta}$ nanocrystals on graphene as a synergistic catalyst for rechargeable zinc-air batteries. Sustain. Mater. Technol. 29 https://doi.org/10.1016/j.susmat.2021.e00282.